SAE International	SURFACE VEHICLE INFORMATION REPORT	SAE J2868 OCT2010 Issued 2010-10

Pedestrian Dummy Full Scale Test Results and Resource Materials

RATIONALE

Not applicable.

FOREWORD

Worldwide, vehicle impacts with pedestrians constitute the most frequent cause of traffic-related fatalities. With this background, the SAE Human Biomechanics and Simulations Standards Steering Committee formed the Pedestrian Dummy Task Force with the goal of developing initial performance specifications for a pedestrian research crash-test dummy which could be used to study the motions and sequence of body component impacts which lead to pedestrian trauma. Additional uses for such a dummy could also include the:

- Study of pedestrian kinematics
- Facilitation of crash reconstruction techniques including pedestrian kinematics
- Assessment of injury probabilities for given vehicle, crash, and countermeasure combinations
- Design of countermeasures
- Evaluation of active systems (pop-up hoods, airbags, etc.)
- Refinement of component test parameters and procedures
- Validation of computer simulations

The primary result of the Pedestrian Dummy Task Force was the preparation of SAE J2782 “Performance Specifications for a Midsize Pedestrian Research Dummy”. During the preparation of SAE J2782, the Task Force interacted with several key technical reports which, although not included in J2782, can provide helpful background and test and analysis examples for those working with SAE J2782 or otherwise studying pedestrian safety. These documents and information were collected into this SAE Information Report (SAE J2868) by the SAE Pedestrian Dummy Task Force.

SAENORM.COM : Click to view the full PDF of j2868_201010

SAE Technical Standards Board Rules provide that: “This report is published by SAE to advance the state of technical and engineering sciences. The use of this report is entirely voluntary, and its applicability and suitability for any particular use, including any patent infringement arising therefrom, is the sole responsibility of the user.”
SAE reviews each technical report at least every five years at which time it may be reaffirmed, revised, or cancelled. SAE invites your written comments and suggestions.
Copyright © 2010 SAE International
All rights reserved. No part of this publication may be reproduced, stored in a retrieval system or transmitted, in any form or by any means, electronic, mechanical, photocopying, recording, or otherwise, without the prior written permission of SAE.

TO PLACE A DOCUMENT ORDER: **Tel: 877-606-7323 (inside USA and Canada)**
Tel: +1 724-776-4970 (outside USA)
Fax: 724-776-0790
Email: CustomerService@sae.org
SAE WEB ADDRESS: http://www.sae.org

SAE values your input. To provide feedback on this Technical Report, please visit
http://www.sae.org/technical/standards/j2868_201010

TABLE OF CONTENTS

SAENORM.COM : Click to view the full PDF of j2868_201010

SAENORM.COM : Click to view the full PDF of j2868_201010

1. SCOPE

The materials included in this J document are not intended to represent a complete summary of pedestrian safety research activities, but are rather a collection of materials which can be helpful to users of SAE J2782.

2. REFERENCES

2.1 Applicable Documents

The following publications form a part of this specification to the extent specified herein. Unless otherwise indicated, the latest issue of SAE publications shall apply.

2.1.1 SAE and Stapp Publications

Available from SAE International, 400 Commonwealth Drive, Warrendale, PA 15096-0001, Tel: 877-606-7323 (inside USA and Canada) or 724-776-4970 (outside USA), www.sae.org.

Pritz, H. B., (1978), Comparison of the Dynamic Responses of Anthropomorphic Test Devices and Human Anatomic Specimens in Experimental Pedestrian Impacts, Proceedings of the 22nd Stapp Car Crash Conference.

Eppinger, R. H., Marcus, J. H., Morgan, R. M., (1984), Development of Dummy and Injury Index for NHTSA's Thoracic Side Impact Protection Research Program, SAE 840885.

SAE J211-1 Instrumentation for Impact Test - Part 1 - Electronic Instrumentation

SAE J2782 Performance Specifications for a Midsize Male Pedestrian Research Dummy

SAE CAESAR Harrison, C. R., Robinette, K. M., (2002), Summary Statistics for the Adult Population (Ages 18-65) of the United States of America, Interim Report: AFRL-HE-WP-TR-2002-0170.

2.1.2 ESV Publications

Available from NHTSA, National Highway Traffic Safety Administration, 1200 New Jersey Avenue, SE, West Building, Washington, D.C. 20590, USA, www.nhtsa.gov.

ESV 131-O Fredriksson, R., Haland, Y., Yang, J., (2001), Evaluation of a New Pedestrian Head Injury Protection System with a Sensor in the Bumper and Lifting of the Bonnet's Rear Part, Proceedings of the 17th International Technical Conference on the Enhanced Safety of Vehicles

ESV 463-O Akiyama, A., Okamoto, M., Rangarajan N., (2001), Development and Application of the New Pedestrian Dummy, Proceedings of the 17th International Technical Conference on the Enhanced Safety of Vehicles

ESV 05-0280-O Takahashi, Y., Kikuchi, Y., Okamoto, M., Akiyama, A., Ivarsson, J., Bose, D., Subit, D., Crandall, J., 2005 ESV, Biofidelity Evaluation for the Knee and Leg of the Polar Pedestrian Dummy

ESV 05-0394 Kerrigan, J.R., Murphy, D., Drinkwater, D.C., Kam, C.Y., Bose, D., Crandall, J.R., 2005 ESV, Kinematic Corridors for PMHS Tested in Full-Scale Pedestrian Impact Tests

ESV 09-0505 Scherer, R., et al., 2009 ESV, WorldSID Production Dummy Biomechanical Responses

SAENORM.COM : Click to view the full PDF of j2868_201010

2.1.3 ISO Publications

Available from International Organization for Standardization, 1 rue de Varembe, Case Postale 56, CH-1211 Geneva 20, Switzerland, Tel: +41-22-749-01-11, www.iso.org.

ISO/DIS 13232-4 Motorcycles—Test and analysis procedures for research evaluation of rider crash protective devices fitted to motorcycles—Part 4: Variables to be measured, instrumentation, and measurement procedures

ISO/DIS 13232-5 Motorcycles—Test and analysis procedures for research evaluation of rider crash protective devices fitted to motorcycles—Part 5: Injury indices and risk/benefit analysis

ISO/TR-9790:1999(E) Road Vehicles—Anthropomorphic side impact dummy—Lateral impact response requirements to assess the biofidelity of the dummy

ISO-15830(all parts):2005(E) Road vehicles — Design and performance specifications for the WorldSID 50th percentile male side impact dummy

2.1.4 SAFE Publication

Available from SAFE Association, P.O. Box 130, Creswell, OR 97426-0130, Tel: 541-895-3012, www.safeassociation.com.

White, R., Rangarajan, N., Haffner, M., (1996), Development of the THOR Advanced Frontal Crash Test Dummy, Proceedings of the 34th SAFE Association Annual Symposium, pp. 122-135

2.1.5 UMTRI Publication

Available from University of Michigan Transportation Research Institute, 2901 Baxter Road, Ann Arbor, MI 48109-2150, Tel: 734-764-6504, www.umtri.umich.edu.

Schneider, L. W., Robbins, D. H., Pflug, M. A., Snyder, R. G., (1983) Anthropometry of Motor Vehicle Occupants, Vol 1: Procedures, Summary Findings and Appendices, Final Report, UMTRI-83-53-1.

2.1.6 Other Publications

Chandler, R. F., Clauser, C. E., McConville, J. T., Reynolds, H. M., Young, J. W., (March 1975), Investigation of Inertial Properties of the Human Body, AMRL-TR-74-137.

2.2 Related Publications

The following publications are provided for information purposes only and are not a required part of this SAE Technical Report.

2.2.1 SAE and Stapp Publications

Available from SAE International, 400 Commonwealth Drive, Warrendale, PA 15096-0001, Tel: 877-606-7323 (inside USA and Canada) or 724-776-4970 (outside USA), www.sae.org.

SAE J211-2 Instrumentation for Impact Test - Part 2 - Photographic Instrumentation

Cavanaugh, J.M., Nyquist, G.W., Goldberg, S.J., King, A.I., "Lower Abdominal Tolerance and Response," SAE Technical Paper 861878, 1986, doi:10.4271/861878.

Daniel, R.P., Irwin, A., Athey, J., Balser, J. et al., "Technical Specifications of the SID-IIs Dummy," SAE Technical Paper 952735, 1995, doi:10.4271/952735.

SAENORM.COM : Click to view the full PDF of j2868_201010

Irwin, A. and Mertz, H.J. "Biomechanical Basis for the CRABI and Hybrid III Child Dummies," SAE Technical Paper 973317, 1997, doi:10.4271/973317.

Irwin, A., Mertz, H. J., Elhagediab, A. M., Moss, S., (2002) Guidelines for Assessing Biofidelity of Side Impact Dummies of Various Sizes and Ages, Stapp Car Crash Journal, Vol. 46.

Ishikawa, H. Kajzer, J., Ono, K., Sakurai, M. (1994) Simulation of Car Impact to Pedestrian Lower Extremity: Influence of Different Car-Front Shapes and Dummy Parameters on Test Results. Accident Analysis and Prevention 26(2), pp. 231-242.

Kajzer, J., Matsui, Y., Ishikawa, H., Schroeder, G. et al., "Shearing and Bending Effects at the Knee Joint at Low Speed Lateral Loading," SAE Technical Paper 1999-01-0712, 1999, doi:10.4271/1999-01-0712.

Kajzer, J., Schroeder, G., Ishikawa, H., Matsui, Y. et al., "Shearing and Bending Effects at the Knee Joint at High Speed Lateral Loading," SAE Technical Paper 973326, 1997, doi:10.4271/973326.

Maltese, M. R., Eppinger, R. H., Rhule, H., Donnelly, B., Pintar, F. A., Yoganandan, N., (2002) Response Corridors of Human Surrogates in Lateral Impacts, Stapp Car Crash Journal 46, pp. 321-351.

Matsui, Y., (2001) Legform Impactor and Injury Tolerance of the Human Leg in Lateral Impact, Stapp Car Crash Journal 45, pp. 495-509.

Mertz, H. J., "A Procedure for Normalizing Impact Response Data," SAE Technical Paper 840884, 1984, doi:10.4271/840884.

Mertz, H.J., Irwin, A.L., Melvin, J.W., Stanaker, R.L. et al., "Size, Weight and Biomechanical Impact Response Requirements for Adult Size Small Female and Large Male Dummies," SAE Technical Paper 890756, 1989, doi:10.4271/890756.

Morgan, R.M., Marcus, J.H., and Eppinger, R.H., "Side Impact - The Biofidelity of NHTSA's Proposed ATD and Efficacy of TTI," SAE Technical Paper 861877, 1986, doi:10.4271/861877.

Nyquist, G.W., Cheng, R., El-Bohy, A.A.R., and King, A.I., "Tibia Bending: Strength and Response," SAE Technical Paper 851728, 1985, doi:10.4271/851728.

2.2.2 Government Publications

Available from NHTSA, National Highway Traffic Safety Administration, 1200 New Jersey Avenue, SE, West Building, Washington, D.C. 20590, www.nhtsa.gov.

[2006] 49CFR572.34PART 572_ANTHROPOMORPHIC TEST DEVICES—Subpart E_Hybrid III Test Dummy—THORAX

Available from Anthropology Research Project, Inc., 503 Xenia Avenue, Yellow Springs, OH 45387.

Gordon, C., Churchill, T., Clauser, C., Bradtmillter, B., McConville, J., Tebbetts, I., Walker, R. (1988) Anthropometric Survey of U.S. Army Personnel: Summary Statistics Interim Report, NATICK/TR-89/027.

SAENORM.COM : Click to view the full PDF of j2868_201010

2.2.3 ESV Publications

Available from NHTSA, National Highway Traffic Safety Administration, 1200 New Jersey Avenue, SE, West Building, Washington, D.C. 20590, USA, www.nhtsa.gov.

Detweiler, D. T., Miller, R. A., (2001) Development of a Sport Utility Front Bumper System for Pedestrian Safety and 5 mph Impact Performance, Proceedings of the 17th International Technical Conference on the Enhanced Safety of Vehicles, ESV 145-W.

Harris, J., Grew, N. D., (1985) The Influence of Car Design on Pedestrian Protection, Proceedings of the 10th International Technical Conference on the Experimental Safety Vehicles.

Mizuno, Y., Summary of IHRA Pedestrian Safety WG Activities (2003)—Proposed Test Methods to Evaluate Pedestrian Protection Afforded by Passenger Cars, Proceedings of the 18th International Technical Conference on the Enhanced Safety of Vehicles, ESV 580-O.

Nagatomi, K., Akiyama, A., Kobayashi, T., (1996) Bumper Structure for Pedestrian Protection, Proceedings of the 15th International Technical Conference on the Enhanced Safety of Vehicles, ESV 96-S4-O-02.

Shaw, G., Lessley, D., Kent, R., Crandall, J., (2005) Dummy Torso Response to Anterior Quasi-Static Loading, Proceedings of the 19th International Technical Conference on the Enhanced Safety of Vehicles, ESV 05-0371-O.

2.2.4 IRCOBI Publications

Available from IRCOBI Secretariat, c/o AGU Zurich, Winkelriedstrasse 27 - CH-8006 Zurich, Switzerland www.ircobi.org.

Ishikawa, H. Kajzer, J., Ono, K., Sakurai, M., Simulation of Car Impact to Pedestrian Lower Extremity: Influence of Different Car-Front Shapes and Dummy Parameters on Test Results, Proceedings of the 1992 International Research Conference on Biokinetics of Impacts.

Kajzer, J., Cavallero, C., Bonnoit, J., Morjane, A., Ghanouchi, S., Response of the Knee Joint in Lateral Impact: Effect of Bending Moment, Proceedings of the 1993 International Research Conference on Biokinetics of Impacts Conference.

Matsui, Y., Ishikawa, H., Sasaki, A., Kajzer, J., Schroeder, G., Impact Response and Biofidelity of Pedestrian Legform Impactors, Proceedings of the 1999 International Research Conference on Biokinetics of Impacts Conference, pp. 343-354.

Ramet, M., Bouquet, R., Bermond, F., Caire, Y., Shearing and Bending of The Human Knee Joint Tests in Quasi-Static Lateral Load, Proceedings of the 1995 International Research Conference on Biokinetics of Impacts Conference, pp. 93-105.

SAENORM.COM : Click to view the full PDF of j2868_201010

2.2.5 Other Publications

Ballesteros, M. F., Dischinger, P. C., Langenberg, P. (2004) Pedestrian Injuries and Vehicle Type in Maryland, 1995-1999. Accident Analysis and Prevention 36(1), pp. 73-81.

EEVC Working Group 17 (1998) Improved Test Methods to Evaluate Pedestrian Protection Afforded by Passenger Cars, http://www.eevc.org/publicdocs/WG17_Improved_test_methods.pdf

GESAC, Inc. (2000) Polar-II User's Manual Version 2.2.

2.3 Definitions

2.3.1 ARM

That portion of the upper extremity from the shoulder to the elbow.

2.3.2 FOOT

That portion of the lower extremity from the ankle to the end of the toes.

2.3.3 FOREARM

That portion of the upper extremity from the elbow to the wrist.

2.3.4 HAND

That portion of the upper extremity from the wrist to the finger tips.

2.3.5 IMPACT POINT

The point in space where the vehicle/buck first contacts the pedestrian.

2.3.6 LEG

That portion of the lower extremity from the knee to the ankle.

2.3.7 STUB ARM

A dummy upper extremity which terminates at or proximal to the elbow (i.e., does not include the forearm and the hand).

2.3.8 THIGH

That portion of the lower extremity from the hip to the knee.

2.3.9 VALGUS BENDING

Bending about the fore-aft dummy axis (x).

2.3.10 VULNERABLE ROAD USERS

Terminology used in Global Technical Regulations, European Union regulations, and commonly used in the field of safety research (see ESV session guide) to describe pedestrians, cyclists, and motorcyclists.

SAENORM.COM : Click to view the full PDF of j2868_201010

2.4 Symbols, Subscripts and Abbreviations

2.4.1 Abbreviations

ATD	Anthropomorphic Test Dummy
AMRL	Aerospace Medical Research Lab (see Chandler, 1975)
AMVO	Anthropometry for Motor Vehicle Occupants Database as established by UMTRI-83-53-1
ANSUR	1988 Anthropometric Survey of U.S. Army Personnel as listed in 2.1.6
C1, C2, etc.	Cervical vertebrate number 1, 2, etc.
CAESAR	Civilian American and European Surface Anthropometry Resource as listed in 2.1.1
c.g.	Center of gravity
CV	Coefficient of variation defined as the standard deviation divided by the average
DAS	Data acquisition system, normally consisting of sensors, signal conditioning and Recorders
ESV	Conference on the Enhanced Safety of Vehicles
FMVSS	Federal Motor Vehicle Safety Standard
FPS	Frames per second
IRCOBI	International Research Council on the Biomechanics of Impact
ISO	International Organization for Standardization
MT	Mid-thorax
NHTSA	The National Highway Traffic Safety Administration
PMHS	Post mortem human subject (i.e., cadaver)
SAFE	Survival and Flight Equipment Association
SD	Standard deviation
T1, T8, etc.	Thoracic vertebrate number 1, 2, etc.
THOR	**T**est Device for **H**uman **O**ccupant **R**estraint, an advanced frontal crash test dummy developed by the NHTSA beginning in the 1990s
UMTRI	University of Michigan Transportation Research Institute
US	Upper spine
WorldSID	World Side Impact Dummy

2.4.2 Symbols

2.4.2.1 Vehicle Reference System (fixed with respect to the moving vehicle) (4.8.4.1.2)

x Positive motions are forward with respect to the car
z Positive motions are down
V_r Resultant velocity in the vehicle reference system xz plane

2.4.2.2 Dummy Positioning Reference System (4.8.3) per SAE J211-1

X + forward from dummy
Y + right from dummy
Z + down
t time

2.4.2.3 Imager Frame Reference System (4.8.4.1.2)

x_F + left in the image (assuming the image is of the left side of the car and the rear of the dummy)
z_F + down in the image

SAENORM.COM : Click to view the full PDF of j2868_201010

3. WHOLE BODY KINIMATIC BIOFIDELITY COMPARISONS BETWEEN DUMMY AND PMHS TEST RESULTS

A properly designed and fabricated pedestrian crash test dummy should provide overall impact kinematics which are representative of humans. For example, the trajectory and velocities of a dummy head in a vehicle impact should be similar to what would be expected of a human head in a similar impact. Typically such whole body dummy kinematics are evaluated by making comparisons between dummy and PMHS motions and velocities.

The materials which follow in this section of the document provide the reader with an example of how such kinematic comparison studies can be performed. The procedures are based on test series conducted at the University of Virginia and are described by Kerrigan et al. at the 19th ESV Conference (Kerrigan et al., ESV 2005). The test series included three PMHS tests and three pedestrian dummy tests. All tests were conducted with the pedestrian in an upright posture at a vehicle impact speed of 40 km/h. PMHS motions were scaled as needed to adjust for PMHS height, PMHS motion corridors were determined, a dummy was tested using the PMHS setup and test procedures, and the dummy motions were compared to the PMHS corridors (additional PMHS anthropometry provided in Kerrigan et al., ESV 2005).

3.1 Test Procedures

3.1.1 General Test Setup

The general test setup is shown in Figure 1.

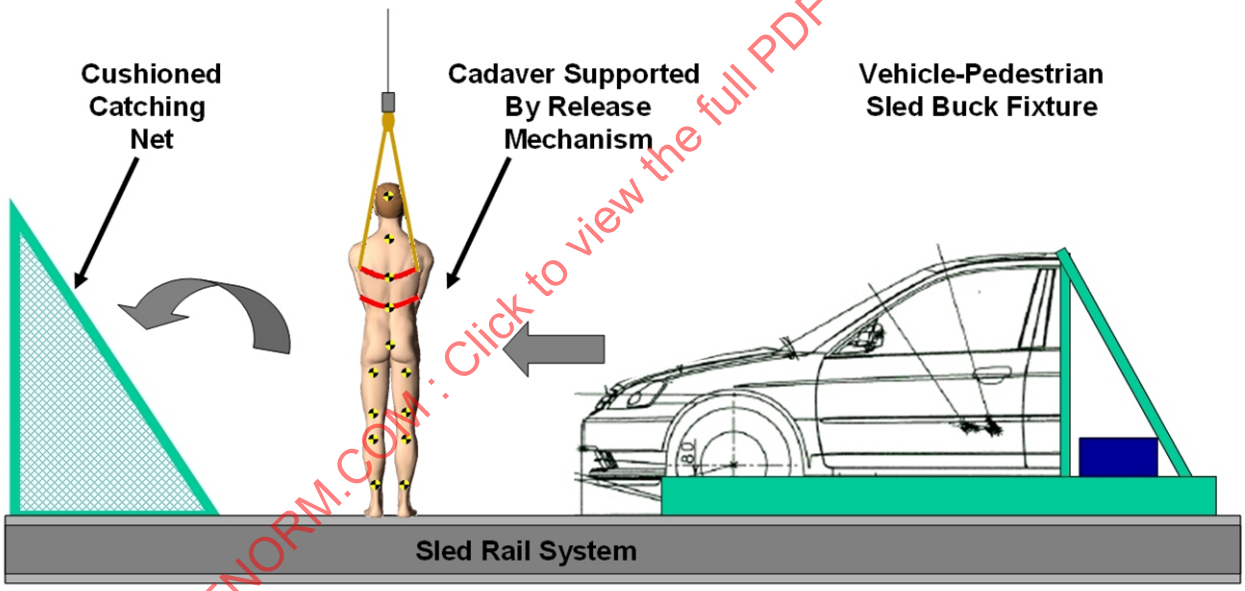

SAENORM.COM : Click to view the full PDF of j2868_201010

FIGURE 1 - GENERAL TEST SETUP

3.1.2 Impact Buck Details

3.1.2.1 Buck Construction

The vehicle used for this example was a 4 Door Honda Civic model year 2004 produced for sale in the U.S. market. For reference the centerline profile of the Civic, which is shown in various included data plots, is found in Table 1 and the geometric locations of specific front end assembly details are found in Figure 2.

TABLE 1 - 2004 CIVIC CENTERLINE PROFILE

X (mm)	Z (mm)
778	0
780	-2
772	-6
762	-6
751	-6
747	-25
720	-29
689	-46
652	-58
287	-133
270	-167
184	-190
182	-208
221	-242
213	-319
167	-346
163	-413
157	-450
155	-490
178	-508
206	-531
223	-562
237	-592
264	-625
300	-671
341	-706
378	-733
433	-748
525	-773
698	-825
815	-858
890	-875
985	-892
1061	-902
1121	-910
1175	-915
1225	-913
1284	-921
1422	-1013
1625	-1140
1800	-1250

SAENORM.COM : Click to view the full PDF of j2868_201010

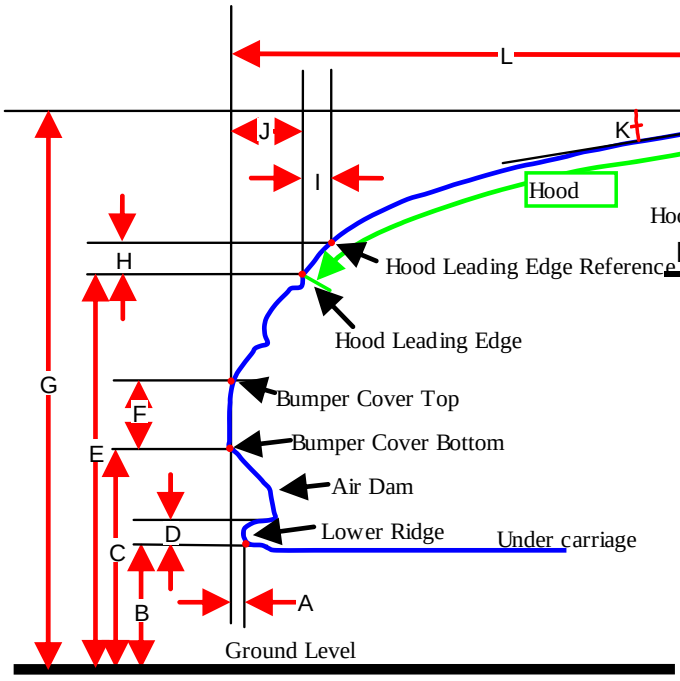

Measurement	Unit	Value
A	mm	28
B	mm	201
C	mm	355
D	mm	45
E	mm	642
F	mm	112
G	mm	912
H	mm	50
I	mm	46
J	mm	119
K	degrees	9
L	mm	980
M	degrees	32

FIGURE 2 - HONDA DETAILS

The vehicle buck included the front half of the vehicle structure, including the B-pillar, and was rigidly mounted to a horizontal sled system with the vehicle suspension components locked so that they did not deflect (Figure 3).

3.1.2.2 Buck Mass

The vehicle buck mass was 1175 kg.

3.1.2.3 Buck Attitude

The vehicle buck was set up to represent the base vehicle attitude with the vehicle side sill parallel to the ground line ±2.5 degrees and the bumper height set with the mid-point of the structural bumper beam at a height of 450 mm ± 10 mm above the ground plane.

SAENORM.COM : Click to view the full PDF of j2868_201010

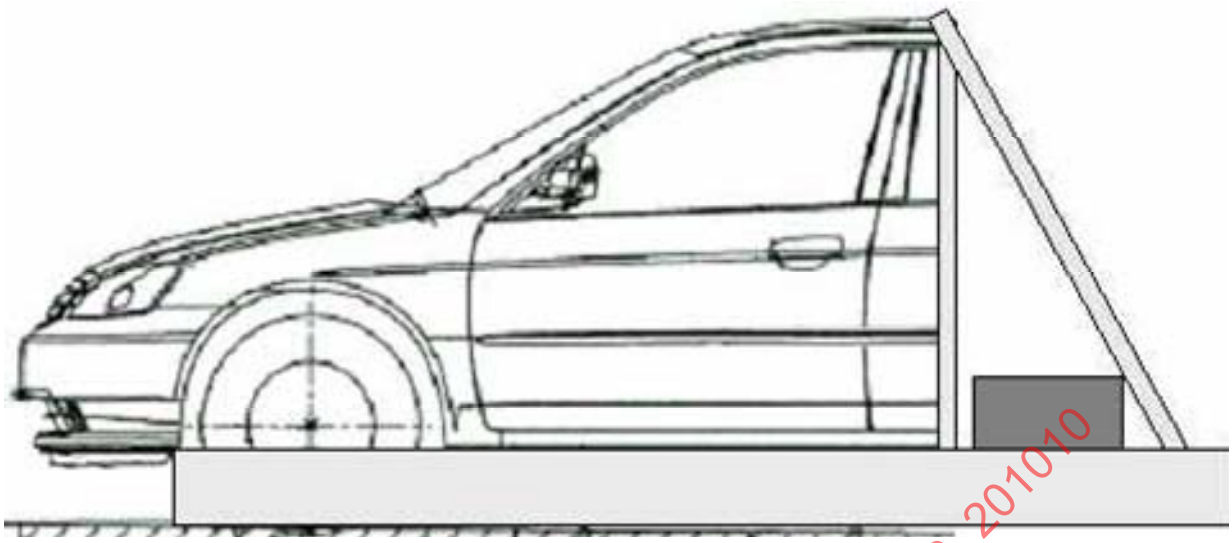

FIGURE 3 - VEHICLE BUCK

3.1.2.4 Buck Condition

The front structure of the vehicle buck was in good condition and was repaired after each test. The structure was constructed out of parts obtained from the original equipment manufacturer and did not include aftermarket replacement parts. Typical replacement parts included the front bumper face, front bumper foam, front grille, hood, hood lock, hood hinges, radiator, condenser, and front bulkhead structure (radiator support).

3.1.3 Impact Speed

The impact velocity for all tests was 40 km/h ± 1 km/h. No vehicle braking occurred until after primary head to vehicle impact.

3.1.4 PMHS Pre-Test Position

PMHS and dummy pre-test positions, support and release for all tests were based on the requirements specified in SAE J2782 Section 4.8.3.

3.1.5 High Speed Cameras and Targets

3.1.5.1 Imaging

For PMHS tests, high speed video was recorded at a frame rate of 1000 Hz, using an off-board imager facing the rear of the PMHS/dummy and the left side of the vehicle (see Figure 1). The field of view stretched horizontally from approximately 47 cm before the impact point to a location approximately 330 cm from the impact point.

3.1.5.2 Photo Targets

Photo targets were dumbbell-type consisting of two 38 mm diameter table tennis balls, painted in contrasting colors, and mounted at both ends of a wooden rod 63.5 mm x 6.35 mm x 6.35 mm. The center point of each target assembly was attached to the outer surface of the PMHS near the location specified in SAE J2782 except at the mid-thorax and head where a single ball was used as a photo target (see Kerrigan et al. ESV 2005 for target attachment details).

SAENORM.COM : Click to view the full PDF of j2868_201010

3.2 Motion Analysis Procedures

3.2.1 PMHS Phototarget Tracking

Motion analysis for all PMHS and dummy tests followed the requirements specified in SAE J2782.

On the PMHS, the motion of the head centroid (henceforth called “head” for convenience) and photo targets at the upper spine (US), mid-thorax (MT), and pelvis reference points were measured. In all cases where a dumbbell type photo target was used, the motion of both balls was tracked. In addition to the photo targets on the surrogate, the motion of a quadrant-type photo target on the vehicle was tracked.

The motion of each photo target was measured by recording the location, in pixels, of each photo target at 4 ms intervals. The first frame that was digitized was about 40 ms prior to t = 0, with t = 0 defined as the time of initial contact between the bumper and the surrogate’s lower extremity.

The point of head strike, determined by visual examination of the video data and confirmed by head mounted accelerometers, was designated as the end of the interval of interest for computing kinematic trajectory and velocity data. The video analysis frame just prior to the time of head strike was determined (Table 2). To prevent the impact altered post impact motions and the position averaging filter from affecting the calculated pre-impact and impact positions and velocities of the head, the x and z coordinates of the head in the 4 ms interval prior to head-to-vehicle impact were used to straight line extrapolate virtual x and z coordinates after head-to-vehicle impact. Such virtual points are unaffected by the impact decelerations.

TABLE 2 - TEST TYPE, TIME OF HEAD STRIKE, DIGITIZED FRAME CLOSEST TO THE TIME OF HEAD STRIKE AND LAST FRAME DIGITIZED FOR EACH TEST IN THE STUDY

Test	Type	Vehicle	Time of Head Strike (ms)	Analysis Frame Closest to Head Strike
001	PMHS	Civic	152	152
002	PMHS	Civic	136	136
003	PMHS	Civic	142	140

SAENORM.COM : Click to view the full PDF of j2868_201010

3.2.2 Data Scaling Analysis

NOTE: For each body region in which two photo targets were digitized (i.e., dumbbell-type photo targets), the x and z coordinates (in the frame coordinate system) of each ball on the photo target were averaged at each analysis frame (4 ms intervals) to obtain the motion of the center of the photo target.

NOTE: The following procedures assume a camera view of the left side of the car and the rear of the PMHS. Reverse left and right directions for test setups with a camera view of the right side of the car and the rear of the PMHS.

For the purpose of the trajectory data manipulation two coordinate systems were defined (the second coordinate system, the vehicle coordinate system, will be defined later). The frame coordinate system is defined by the view of the high speed imager. This coordinate system is fixed with respect to the laboratory. The x_F direction is defined as the horizontal axis of the imager frame and z_F is defined as the vertical axis of the imager frame. Positive x_F is to the left (the vehicle travels in the positive x_F direction) and positive z_F points down. The motions of all of the photo targets were tracked in the frame coordinate system by digitizing the location of the photo target in each analysis frame. The origins for the frame coordinate system were as follows:

$x_F = 0$ corresponds to a vertical line passing through the head centroid, upper spine reference point, mid-thorax reference point, and pelvis reference point. If some alignment error between points exists the line should be located so as to minimize the cumulative X^2 errors.

$z_F = 0$ corresponds to the horizontal surface on which the bottom of the dummy shoes rests prior to impact.

3.2.3 Motion Analysis

Motion analysis proceeded as follows:

a. Identify the image frame which just precedes the first indication of contact between the car bumper and the test subject dummy. This could for example be the last frame prior to the illumination of a contact light or prior to any visible movement or deformation of the test subject. This frame becomes analysis frame 0, and corresponds to t = 0.

b. Identify a series of analysis frames prior to and after frame 0 with a time interval between analysis frames of approximately 4 ms. For example, when using a 1000 FPS video camera every 4th frame prior to and after frame 0 will be an analysis frame. Note that although only every 4th frame is analyzed to provide some motion filtering, the use of 1000 FPS allows a more precise determination of the initial contact time.

c. For each analysis frame, digitize the location of the head, upper spine, mid thorax, and pelvis reference points, and the car side target.

d. In order to obtain the scale factors for the video analysis, reference objects of known size were placed in the XZ planes at the mid-point Y distance of the PMHS and the vehicle from the camera and the length of the objects in pixels was determined. For the specific camera location and resolution used for this series of tests the scale factors (SF) for the test subject and vehicle were as follows:

$$\text{PMHS Scale factor} = 3.695\ \text{mm/pixels}$$
$$\text{vehicle Scale factor} = 3.243\ \text{mm/pixels} \qquad \text{(Eq. 1)}$$

e. The filtering convention specified in ISO 13232-4 (ISO, 2004) was used to smooth the position data. All signals were filtered with four passes of the moving average filter:

$$x_{Fi,f} = \frac{x_{Fi-1} + 2x_{Fi} + x_{Fi+1}}{4}$$
$$z_{Fi,f} = \frac{z_{Fi-1} + 2z_{Fi} + z_{Fi+1}}{4} \qquad \text{(Eq. 2)}$$

where:

$x_{Fi,f}$, $z_{Fi,f}$ are the filtered x_F and z_F position at frame i, in mm
x_{Fi}, z_{Fi} are the unfiltered (or filtered on the previous pass) x_F and z_F positions, in the frame coordinate system at frame i, in mm
i - 1 and i + 1 designate the preceding and next analysis frames

f. Scaling – To provide a basis for comparing dummy kinematics it is common to assume that PMHS specimens are geometrically similar and thus can be geometrically scaled to a reference geometry. The reference geometry chosen was that of the specified midsize adult male in the test striding position (see Table 3). Since the proportional length of PMHS body segments relative to the reference geometry varied among body segments, it was determined that the PMHSs were not geometrically similar and thus an individual scale factor for each body segment trajectory for each PMHS was necessary. Twelve individual scale factors (see Table 4) were calculated to account for the head, upper spine, mid thorax, and pelvis motion for the three PMHSs tested. An example calculation to obtain the mid thorax scale factor in test 002, $\lambda^{MT,002}$, is given as:

$$\lambda^{MT,002} = \frac{s^{MT}}{s^{MT,002}_{z,c}} = 1.0062 \qquad \text{(Eq. 3)}$$

SAENORM.COM : Click to view the full PDF of j2868_201010

where:

s^{MT} , is the midsize adult male mid thorax reference point z location in the test striding position, in mm

$s_{z,c}^{MT,002}$ is the $s_{z,c}$ z location value, in mm, for the mid thorax in test 002

The filtered trajectory data, $x_{Fi,f}$ and $x_{Fi,f}$ (Equation 2), were then multiplied by their respective scale factors to obtain the scaled frame coordinate system trajectories $x^*_{Fi,f}$ and $z^*_{Fi,f}$. All scaled values are indicated with a " * ".

TABLE 3 - MIDSIZE MALE MOTION REFERENCE LOCATION[1)]
IN THE TEST STRIDING POSITION WITH SHOES (SEE J2782 4.8.4.1.1.1)

Reference Point	Z Location
Head	-1659
Upper spine	-1501
Mid thorax	-1352
Pelvis	-1005

1) Note that these dimensions are for motion reference points only and are not based on target locations for any particular dummy. Nor are they necessarily key anthropometry locations (see J2782 4.8.4.1.1.1)

TABLE 4 - SCALE FACTORS USED TO SCALE BODY SEGMENT TRAJECTORIES

	001	002	003
Head	0.9224	0.9869	0.9375
Upper spine	0.8942	0.9729	0.9049
Mid thorax	0.9458	1.0062	0.9642
Pelvis	0.9363	1.0284	0.9576

The scaled positions measured in the frame coordinate system, $x^*_{Fi,f}$ and $z^*_{Fi,f}$, are then calculated by:

$$x^*_{Fi,f} = \lambda x_{Fi,f}$$
$$z^*_{Fi,f} = \lambda z_{Fi,f} \quad \text{(Eq. 4)}$$

where:

λ is the scale factor for a given position and test

g. Time Scale – For the purposes of calculating scaled velocities, and for average/corridor development, the time variable t_i, defined as the time at frame i, had to be scaled as well. However since there are numerous scale factors, an individual signal for the scaled time at frame i, t^*_i, had to be calculated for each body region and each test. If the mass density and modulus of elasticity are considered to be constant among the test subjects, the time can be scaled using the length scale factor (Eppinger et al. SAE 1984) so t_i was multiplied by each of the scale factors to obtain each of the t^*_i signals. It should be noted that the use of a single scale factor (based on height for example) for a given test would result in different initial positions for the body region targets when the test data is combined, which would in turn lead to wider motion corridors. See Kerrigan et al., ESV 2005 for further details.

SAENORM.COM : Click to view the full PDF of j2868_201010

h. Transfer the origin of all scaled surrogate photo target position signals to the vehicle reference frame as follows:

$$x_{V,i} = x_{Fi,f} - \left(vx_{F,i,f} - vx_{F,o,f}\right)$$
$$z_{V,i} = z_{Fi,f} - \left(vz_{F,i,f} - vz_{F,o,f}\right) \quad \text{(Eq. 5)}$$

where:

$x_{Fi,f}$, $z_{Fi,f}$ are the filtered x_F and z_F position of each of the surrogate photo targets at analysis frame i, in mm, in the frame coordinate system

$vx_{F,i,f}$, $vz_{F,i,f}$ are the filtered x_F and z_F positions of the vehicle photo target at frame i, in mm in the frame coordinate system

$x_{v,i}$, $z_{v,i}$ are the x and z positions of each of the surrogate photo targets at frame i in the vehicle reference coordinate system, in mm

$vx_{F,o,f}$, $vz_{F,o,f}$ are the filtered x and z positions of the vehicle photo target at analysis frame 0, in mm, in the frame coordinate system

The second coordinate system is the vehicle coordinate system. The vehicle coordinate system is fixed to the vehicle, and defined as follows:

– Positive x towards the front of the car
– Positive z down
– x = 0 is the same vertical line as the frame coordinate system at analysis frame 0, but is fixed and moves with the vehicle
– z = 0 is the same horizontal surface as the frame coordinate system at analysis frame 0

NOTE: The vehicle coordinate system moves in the frame coordinate system positive X direction.

i. Velocity Data – Scaled body segment and vehicle velocities in the frame coordinate system were calculated using the methodology recommended in ISO 13232-5 (ISO, 2002). The component velocities in the x and z directions of each body segment were calculated as:

$$V_{x,i} = \frac{x_{i+1} - x_{i-1}}{t_{i+1} - t_{i-1}}$$
$$V_{z,i} = \frac{z_{i+1} - z_{i-1}}{t_{i+1} - t_{i-1}} \quad \text{(Eq. 6)}$$

where:

$V_{x,i}$, $V_{z,i}$ are each photo target's component velocity, in m/s, in the x and z directions at frame i, in the frame coordinate system

t_i is the time, in ms, at frame i

$i + 1$ and $i - 1$ designate the next and preceding analysis frames

To properly combine the scaled head velocity in the frame coordinate system and the vehicle velocity in the frame coordinate system requires that the individual velocities be calculated as shown above and then combined to generate head velocities in the vehicle coordinate system as follows:

$$V_{H,x} = V_{H,x_F} - V_{V,x_F}$$
$$V_{H,z} = V_{H,z_F} - V_{V,z_F} \quad \text{(Eq. 7)}$$

SAENORM.COM : Click to view the full PDF of j2868_201010

where:

$V_{H,x}$, $V_{H,z}$ are the head x and z velocities in the vehicle axis system
V_{H,x_F}, V_{H,z_F} are the scaled head x_F and z_F velocities in the frame axis system
V_{V,x_F}, V_{V,z_F} are the vehicle x_F and z_F velocities in the frame axis system

Resultant velocities were computed using the length of the velocity vector defined by the components in Equation 7.

3.3 Corridor Development

3.3.1 Trajectory Corridors

Note that corridors were developed based only on the three PMHS tests. For the purposes of trajectory plotting and corridor development, the time when the surrogate's head first contacts any part of the vehicle (head-strike time), is used to determine the end of the trajectory data. Since the time signal is scaled for the PMHS, the time of head strike , t^*_{hs}, is also scaled and then rounded to the nearest 4 ms interval (Table 5).

TABLE 5 - UNSCALED AND SCALED HEAD STRIKE TIMES FOR EACH BODY REGION IN EACH PMHS TEST AT HEAD STRIKE

		Scaled Time at Head Strike t^*_{hs} (ms)		
		001	**002**	**003**
	Un-scaled	152	136	142
Scaled	Head	140	132	132
	Upper spine	136	132	128
	Mid thorax	144	136	136
	Pelvis	144	140	136

Since a different scale factor was used to scale the trajectory of each PMHS body region in each test, the interval of the scaled time signal is different for each PMHS body region in each test. Thus, all of the scaled signals needed to be re-sampled in time to facilitate averaging of the signals.

The average scaled PMHS trajectory was computed by averaging values of each trajectory signal at each of the 4 ms intervals. Averaged scaled trajectories were computed for the head, upper spine, mid thorax, and pelvis and are shown in Figures 12 to 15.

The good repeatability seen in the scaled trajectory plots for the three PMHS tests made traditional corridors based on standard deviations unacceptably small. As a result, it was decided to construct corridors around the means using a percentage of the path length traveled by the object in the vehicle coordinate systems where the path length S is calculated as:

$$S_i = \sum_{j=1}^{i} \sqrt{\left(\bar{x}^*_j - \bar{x}^*_{j-1}\right)^2 + \left(\bar{z}^*_j - \bar{z}^*_{j-1}\right)^2} \qquad \text{(Eq. 8)}$$

where:

S_i is the total path length of the trajectory measured up to frame i, in mm
$\bar{x}^*_j$, and $\bar{z}^*_j$, are the average scaled x and z components of each body segment's trajectory, in mm

SAENORM.COM : Click to view the full PDF of j2868_201010

Four signals were calculated to determine the corridors. These four signals represent the corners of a square, with a reference point on the average trajectory curve, and whose dimension is equal to $(J+k)S_i$, where J and k are variables representing a percentage of the trajectory's path length S_i. The four signals were calculated as:

$$C^{+}_{x,i} = \bar{x}^{*}_{i} + kS_i$$
$$C^{-}_{x,i} = \bar{x}^{*}_{i} - JS_i$$
$$C^{+}_{z,i} = \bar{z}^{*}_{i} + kS_i$$
$$C^{-}_{z,i} = \bar{z}^{*}_{i} - JS_i \qquad \text{(Eq. 9)}$$

where:

$C^{+}_{x,i}$, $C^{-}_{x,i}$, $C^{+}_{z,i}$, $C^{-}_{z,i}$ are the x and z corridor signals for the 4 corners of the percentage path length square

Due to the downward concavity of the average trajectory signals, the negative x motions, and the definition of the $+z$ axis (as down), the kinematic response corridors for the head, upper spine, and mid thorax trajectories were developed by plotting $C^{-}_{x,i}$ vs. $C^{-}_{z,i}$ (for the upper bound) and $C^{+}_{x,i}$ vs. $C^{+}_{z,i}$ (for the lower bound). Since the pelvis average scaled trajectory is concave up, the upper bound of the pelvis corridor was developed by plotting $C^{+}_{x,i}$ vs. $C^{-}_{z,i}$, and the lower bound was developed by plotting $C^{-}_{x,i}$ vs. $C^{+}_{z,i}$.

Based on a review of existing dummy specifications and certification procedures, the total corridor width was set to be 15% of the path length. The choice of 15% was based on a review of the data and was determined not to be overly wide so as to include all dummies, but was wide enough that some level of existing technology could fit within the corridor.

To investigate where the trajectories of the midsize male would lie relative to the test results, several studies were carried out to investigate the influence of the height and related parameters (e.g., increased mass moment of inertia and height of the c.g.) were considered to affect the trajectories (see Appendix E). These studies revealed that the head, upper thoracic spine, and mid-thoracic spine trajectories would most likely fall below (i.e., would result in a lower Z location for a given X displacement) the available PMHS test results and that the pelvis trajectory would most likely be higher (higher Z for a given X). Although the direction of the shift of the trajectory plot for midsize male PMHS tests was apparent (see Appendix E), because of the limited data, it was not possible to quantify the amount of trajectory shift which might be expected for the midsize male.

Based on the theory that midsize male trajectories would lie under the trajectories of the tall PMHS tests, it was decided that the corridor should be asymmetric with an upper bound of 5% of the path length and a lower bound of 10% of the path length from the average trajectories for the head, upper thoracic spine, and mid-thoracic spine. For the pelvis, the corridor was set to have a 10% upper and 5% lower bound. For additional details on the determination of corridors based on path length see Kerrigan et al., ESV 2005.

As discussed above, the head, upper spine and mid thorax corridors were determined using +5% and -10% path length values and the pelvis corridor was based on +10% and -5% path length values. The corridors for the head, upper spine, mid thorax, and pelvis along with the individual PMHS responses and the average PMHS response are shown in Figures 4 to 7. To facilitate implementation, the corridors were defined using piecewise linear boundary segments. A comparison of the average based corridors and the linearized corridors are shown in Figures 8 to 11. The piecewise linear corridors alone are shown in Figures 12 to 15 and quantified in Tables 6 to 9.

SAENORM.COM : Click to view the full PDF of j2868_201010

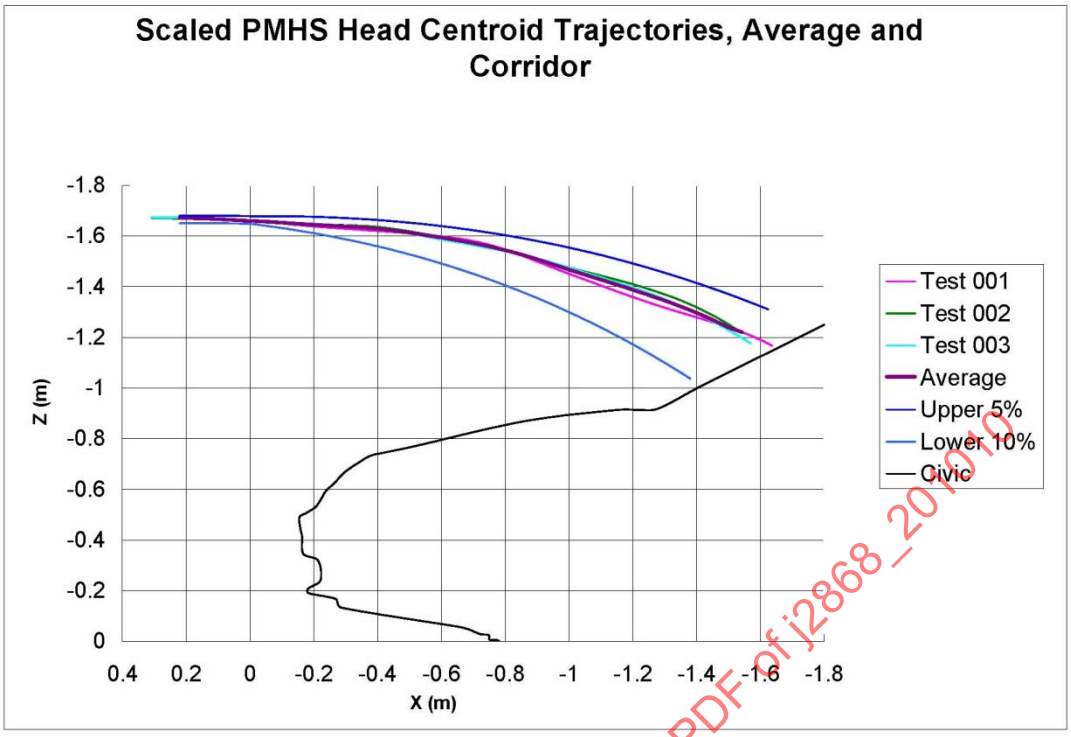

FIGURE 4 - PMHS HEAD CENTROID TRAJECTORY AND CORRIDOR

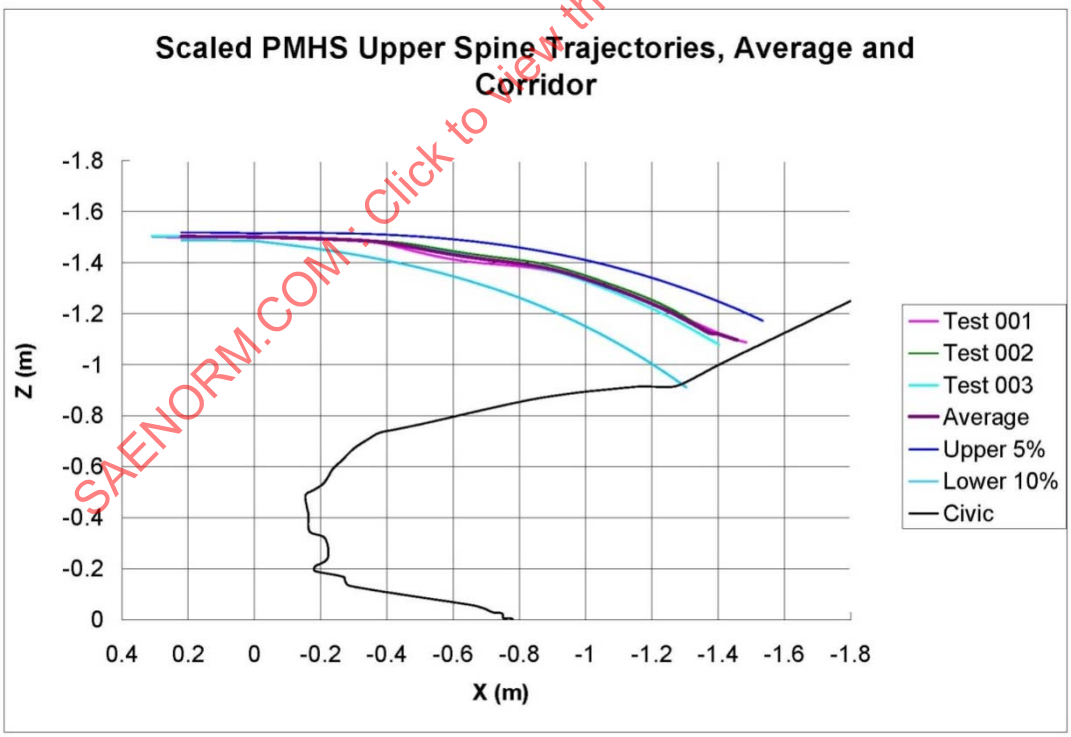

FIGURE 5 - PMHS UPPER SPINE TRAJECTORY AND CORRIDOR

SAENORM.COM : Click to view the full PDF of j2868_201010

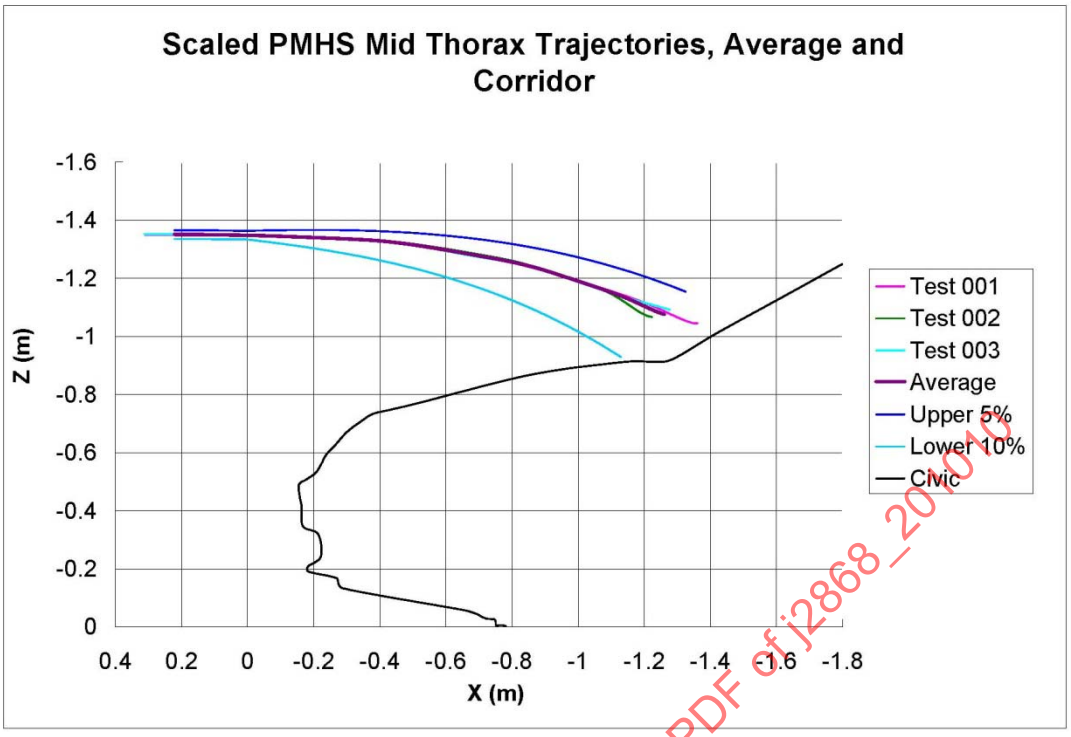

FIGURE 6 - PMHS MID THORAX TRAJECTORY AND CORRIDOR

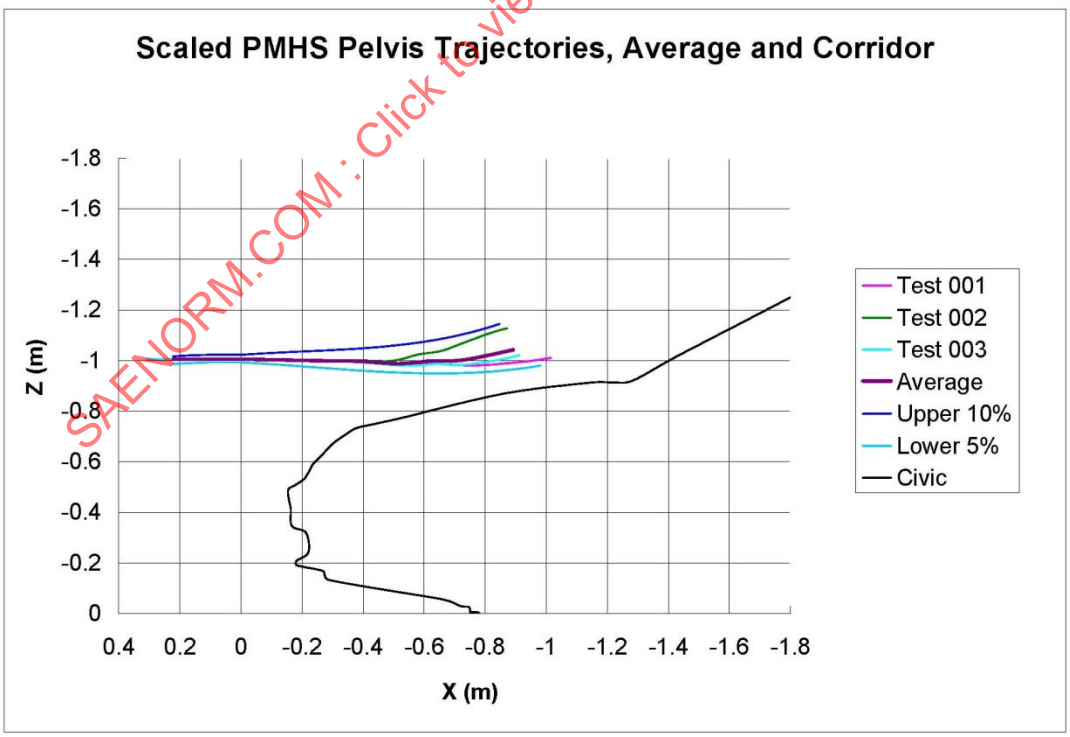

FIGURE 7 - PMHS PELVIS TRAJECTORY AND CORRIDOR

SAENORM.COM : Click to view the full PDF of j2868_201010

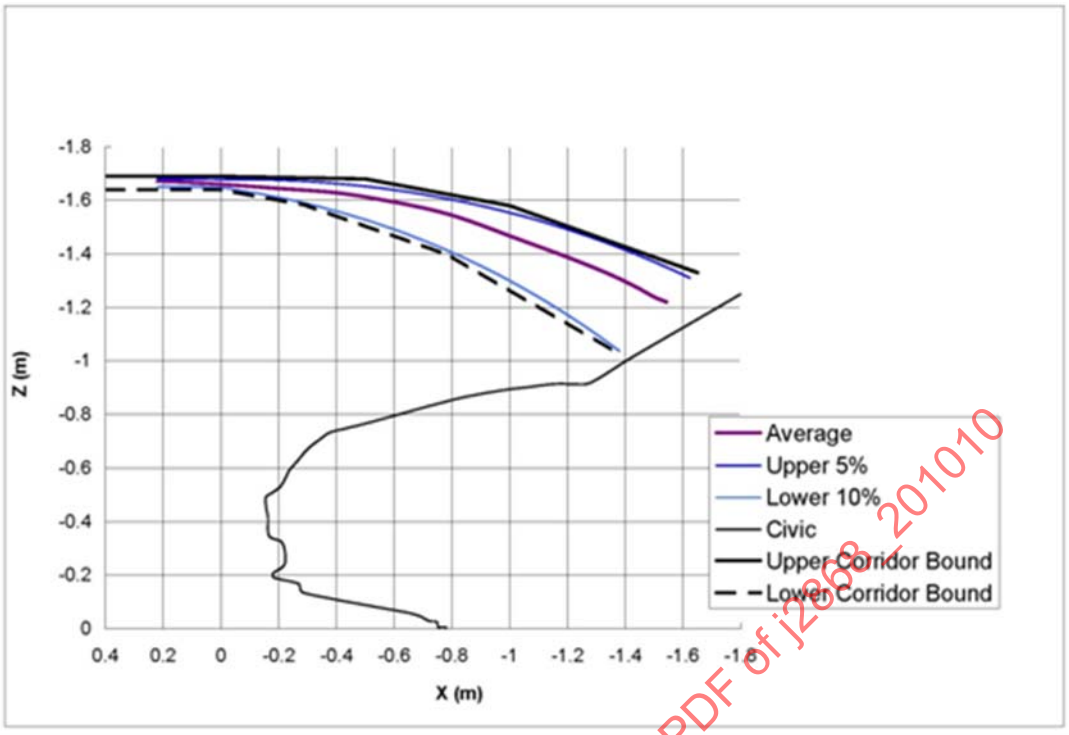

FIGURE 8 - HEAD CENTROID TRAJECTORY AVERAGE CORRIDOR VS PIECEWISE LINEAR

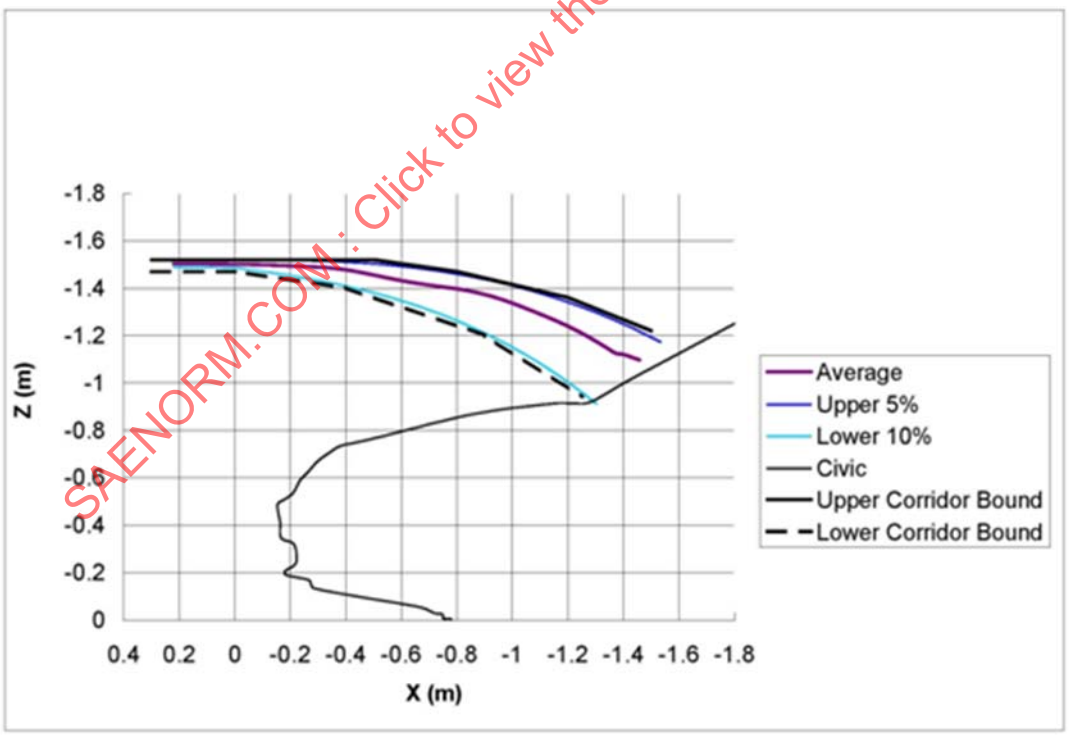

FIGURE 9 - UPPER SPINE TRAJECTORY AVERAGE CORRIDOR VS PIECEWISE LINEAR

SAENORM.COM : Click to view the full PDF of j2868_201010

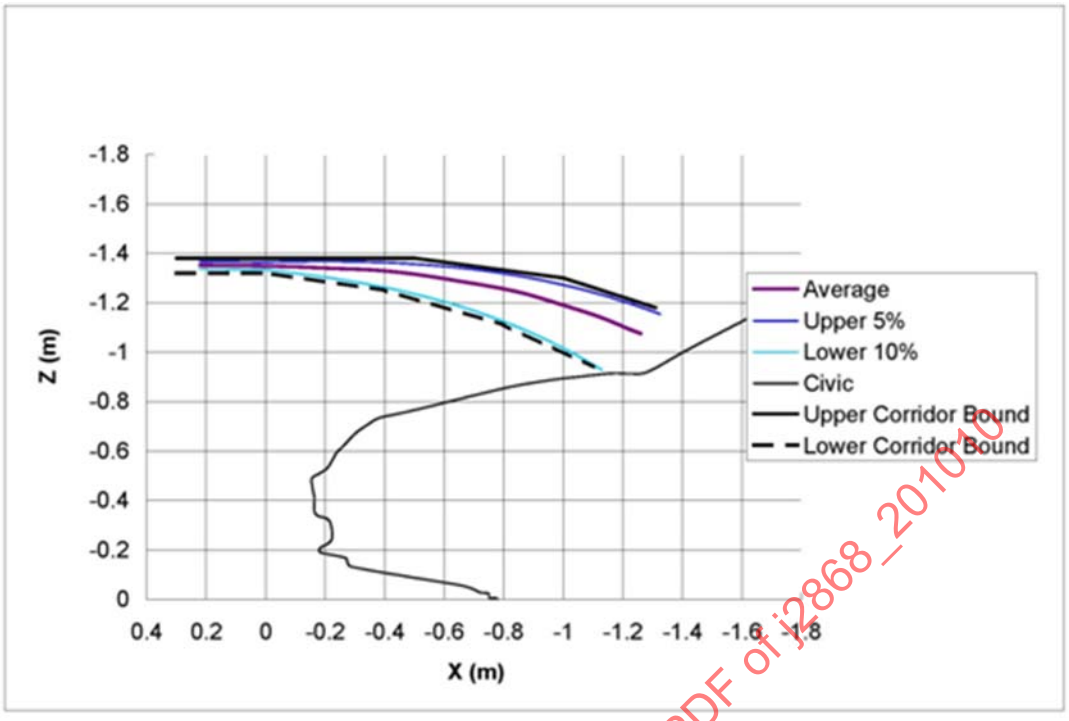

FIGURE 10 - MID THORAX TRAJECTORY AVERAGE CORRIDOR VS PIECEWISE LINEAR

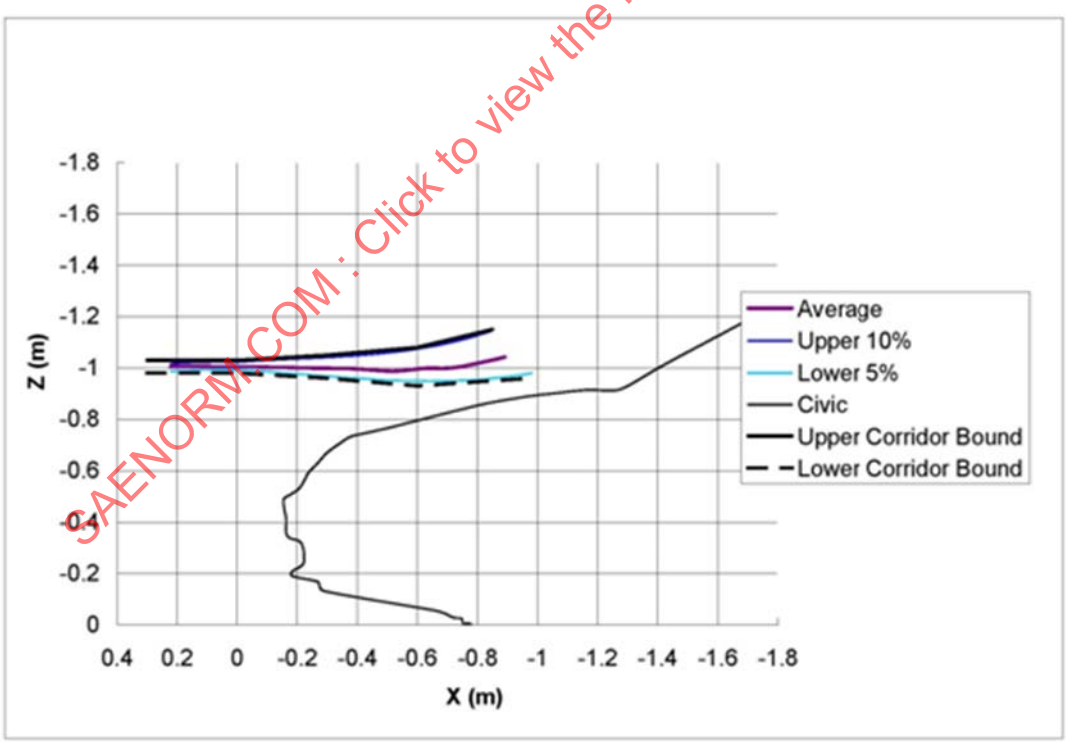

FIGURE 11 - PELVIS TRAJECTORY AVERAGE CORRIDOR VS LINEAR

SAENORM.COM : Click to view the full PDF of j2868_201010

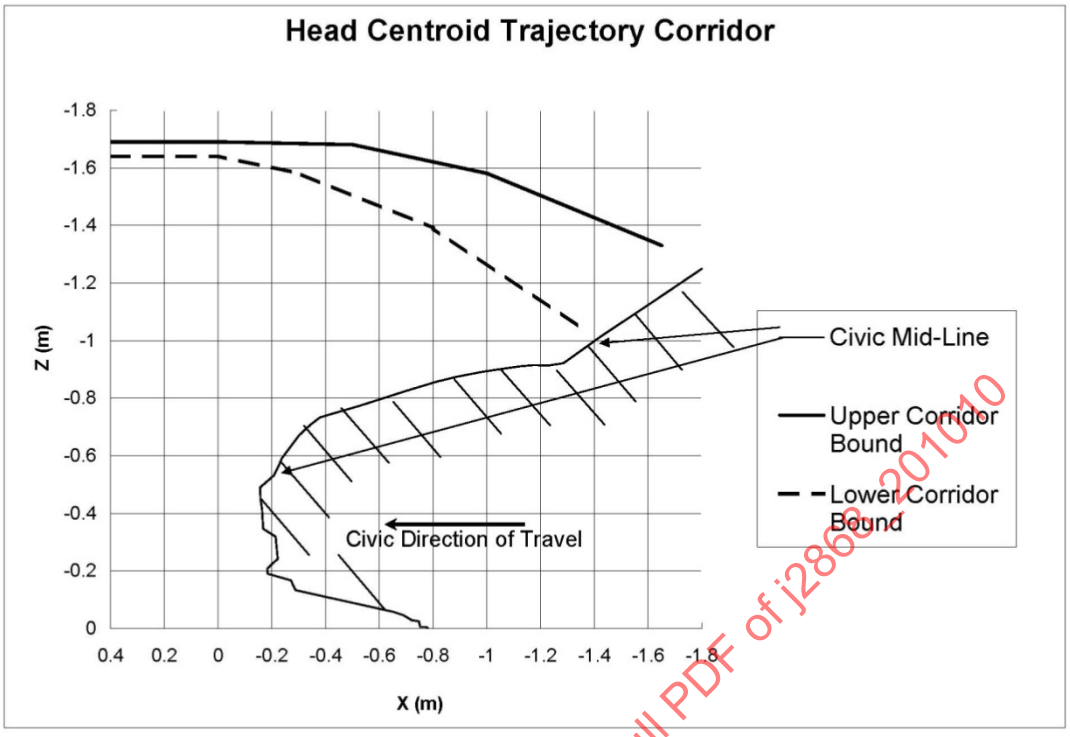

FIGURE 12 - HEAD CENTROID TRAJECTORY CORRIDOR
(IN VEHICLE REFERENCE FRAME)

NOTE: The head centroid displacement corridor above can be plotted with the values in Table 6.

TABLE 6 - HEAD CENTROID TRAJECTORY CORRIDOR

Point	Upper Bound		Lower Bound	
	x(m)	z(m)	x(m)	z(m)
1	0.400	-1.690	0.400	-1.640
2	0	-1.690	0	-1.640
3	-0.500	-1.680	-0.300	-1.580
4	-1.000	-1.580	-0.800	-1.390
5	-1.650	-1.330	-1.370	-1.030

SAENORM.COM : Click to view the full PDF of j2868_201010

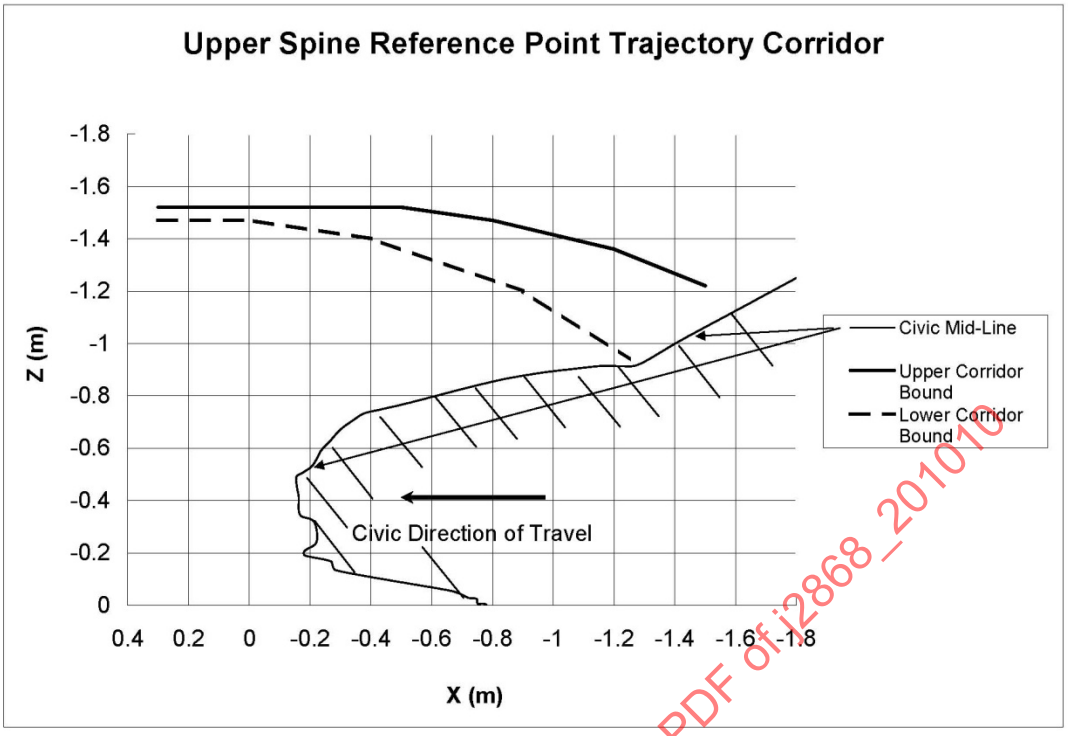

FIGURE 13 - UPPER SPINE REFERENCE POINT TRAJECTORY CORRIDOR
(IN VEHICLE REFERENCE FRAME)

NOTE: The upper spine reference point displacement corridor can be plotted with the values in Table 7.

TABLE 7 - UPPER SPINE REFERENCE POINT DISPLACMENT CORRIDOR

Point	Upper Bound		Lower Bound	
	x(m)	z(m)	x(m)	z(m)
1	0.300	-1.520	0.300	-1.470
2	-0.500	-1.520	0	-1.470
3	-0.800	-1.470	-0.400	-1.400
4	-1.200	-1.360	-0.900	-1.200
5	-1.500	-1.220	-1.250	-0.940

SAENORM.COM : Click to view the full PDF of j2868_201010

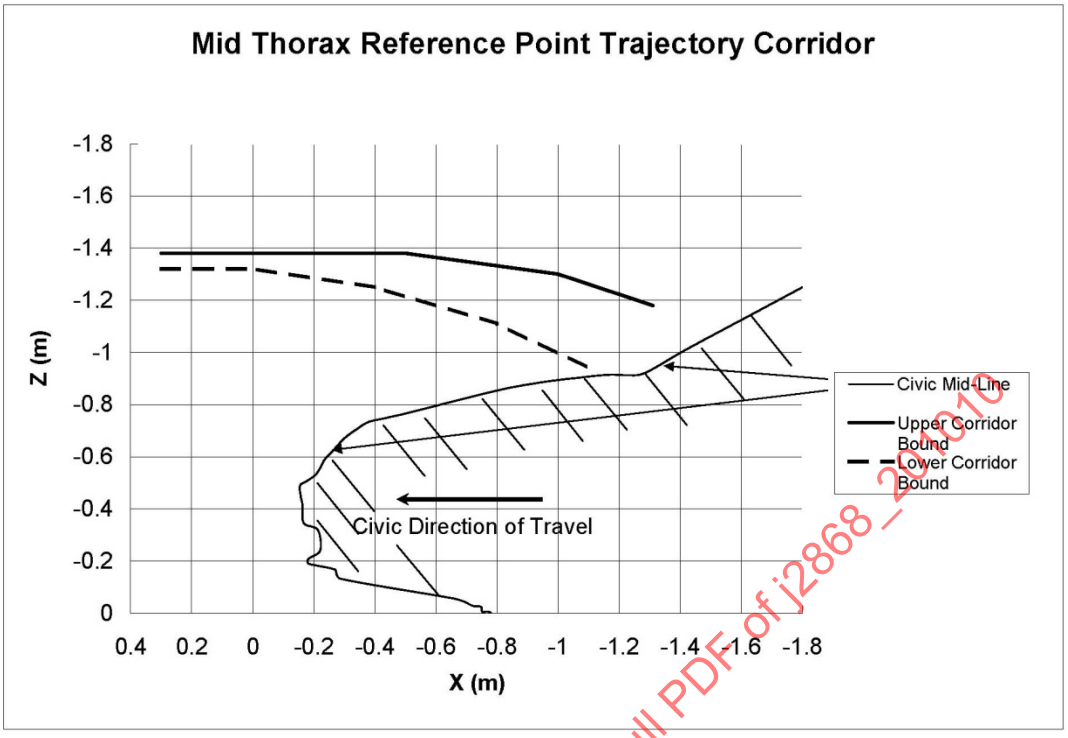

FIGURE 14 - MID-THORAX REFERENCE POINT TRAJECTORY CORRIDOR
(IN VEHICLE REFERENCE FRAME)

NOTE: The mid-thorax reference point trajectory corridor can be plotted with the values in Table 8.

TABLE 8 - MID-THORAX REFERENCE POINT TRAJECTORY CORRIDOR

Point	Upper Bound		Lower Bound	
	x(m)	z(m)	x(m)	z(m)
1	0.300	-1.380	0.300	-1.320
2	-0.500	-1.380	0	-1.320
3	-0.750	-1.340	-0.400	-1.250
4	-1.000	-1.300	-0.800	-1.110
5	-1.310	-1.180	-1.100	-0.940

SAENORM.COM : Click to view the full PDF of j2868_201010

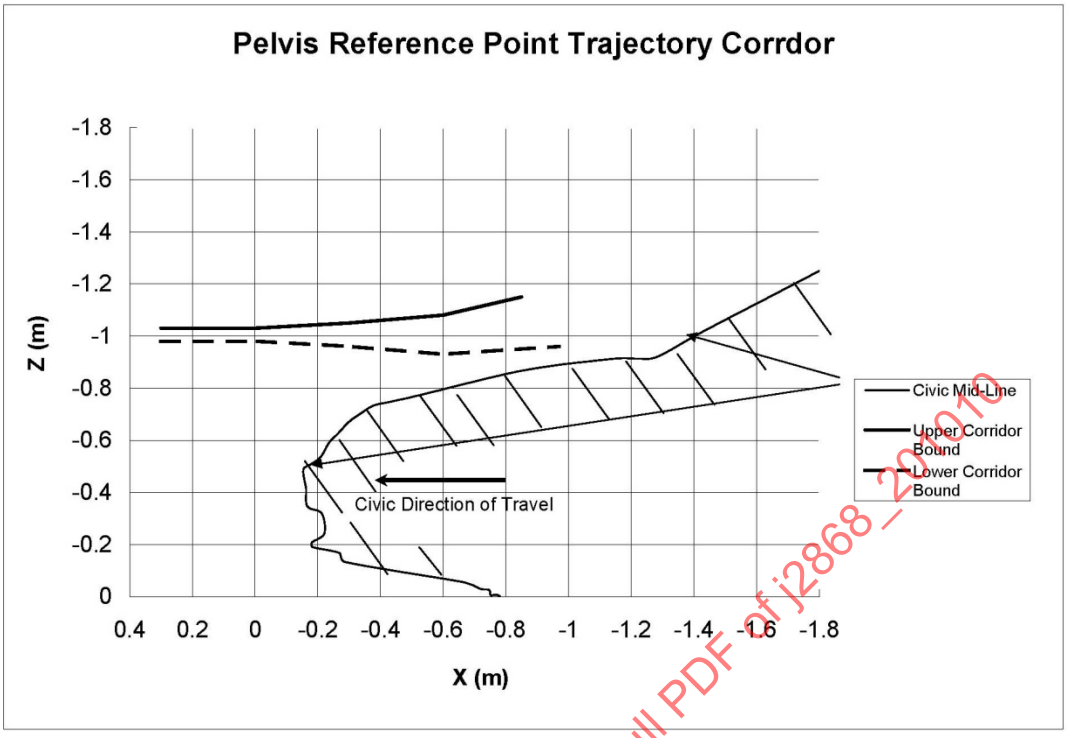

FIGURE 15 - PELVIS REFERENCE POINT TRAJECTORY CORRIDOR
(IN VEHICLE REFERENCE FRAME)

NOTE: The pelvis reference point trajectory can be plotted with the values in Table 9.

TABLE 9 - PELVIS REFERENCE POINT TRAJECTORY CORRIDOR

Point	Upper Bound		Lower Bound	
	x(m)	z(m)	x(m)	z(m)
1	0.300	-1.030	0.300	-0.980
2	0	-1.030	0	-0.980
3	-0.300	-1.050	-0.300	-0.960
4	-0.600	-1.080	-0.600	-0.930
5	-0.850	-1.150	-0.970	-0.960

SAENORM.COM : Click to view the full PDF of j2868_201010

3.3.2 Head Velocity Corridor

The development of the head velocity versus time corridor involved three distinct steps as follows:

1. Using the film analysis procedures described above, the head resultant velocity plots in the vehicle coordinate frame for the three PMHS tests were determined. The three PMHS head resultant velocity plots were averaged for a given time and ± 1 standard deviation corridors were calculated as shown in Figure 16.

2. A review of the three PMHS test videos showed that as expected, the PMHS exhibited no active muscle tension in the neck and thus the head motion was likely not representative of a living pedestrian. To investigate the effect that the lack of neck muscle tension might have on head motion, the motion analysis of a virtual head point was performed.

A virtual head point supported from the PMHS upper spine was mathematically constructed and tracked via film analysis. As shown in Figure 17 the virtual head point, which was rigidly attached to the PMHS upper spine did not move as a result of neck flexibility. The motions of this virtual head point represented the motions of the head which would have occurred had it been supported by a rigid neck. The three PMHS virtual head velocity plots were averaged for a given time and ± 1 standard deviation corridors were calculated as shown in Figure 18.

A comparison of the "rigid" neck and "flexible" neck velocity curves shows some similarity, however, the rigid neck tends to increase the head velocity and it further tends to reduce the time of peak V_r.

3. Recognizing that the actual head velocity for an impacted live human would probably fall somewhere between the "flexible" neck exhibited by the PMHS, and the "rigid" neck, the specified head velocity vs. time corridor was established as follows:

$$\text{Upper corridor} = \text{Max}\left(\text{PMHS}_{\text{avg}} + 1\text{SD}, \text{Virtual}_{\text{avg}} + 1\text{SD}\right)$$
$$\text{Lower corridor} = \text{Min}\left(\text{PMHS}_{\text{avg}} - 1\text{SD}, \text{Virtual}_{\text{avg}} - 1\text{SD}\right) \quad \text{(Eq. 10)}$$

The resulting corridor and the specified linearized corridor are shown in Figure 19. The linearized corridor alone is shown in Figure 20 and quantified in Table 10.

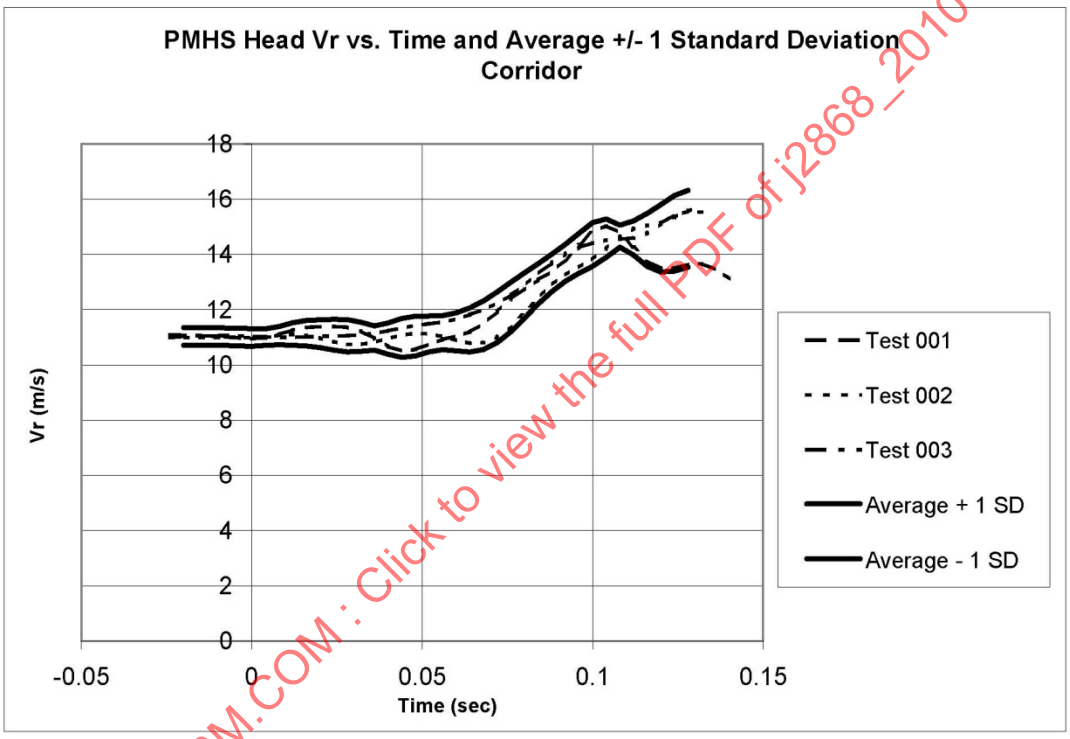

FIGURE 16 - PMHS HEAD VELOCITY ±1 SD CORRIDOR

SAENORM.COM : Click to view the full PDF of j2868_201010

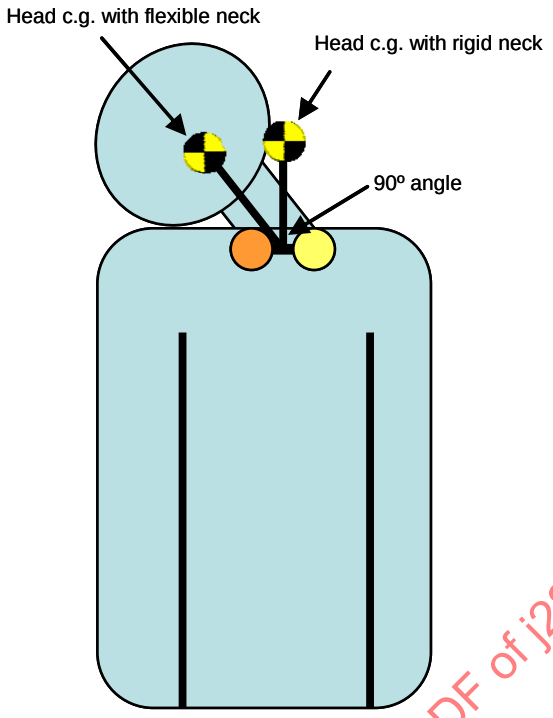

FIGURE 17 - VIRTUAL HEAD WITH RIGID NECK

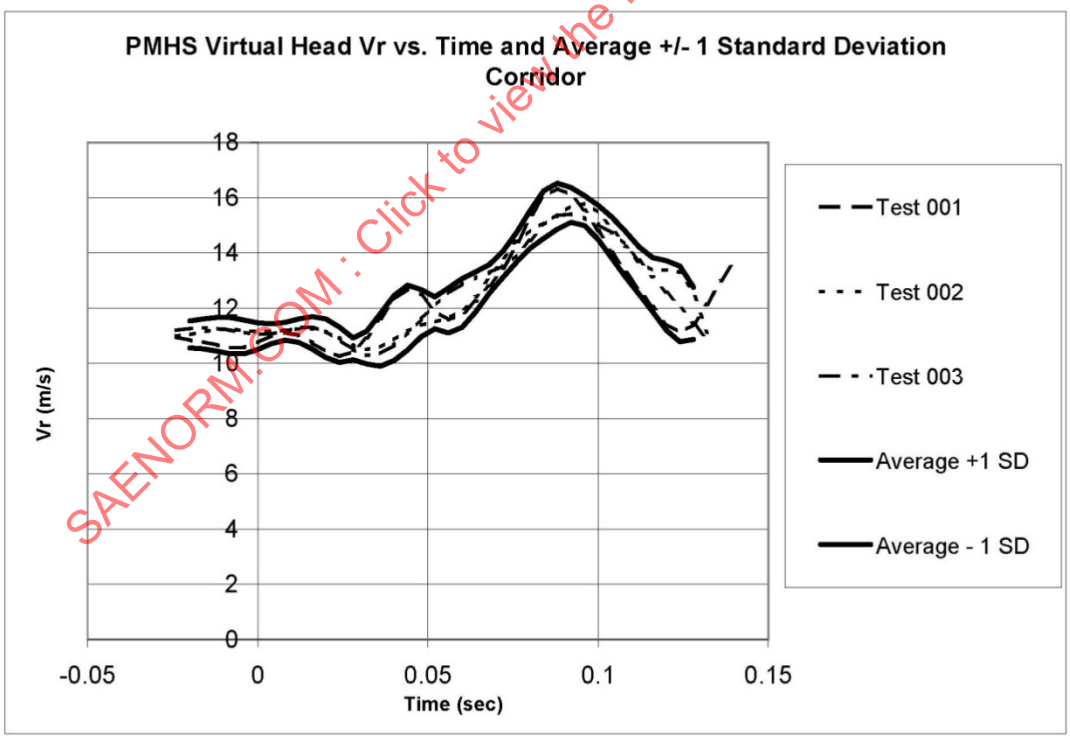

FIGURE 18 - PMHS VIRTUAL HEAD VELOCITY ±1 SD CORRIDOR

SAENORM.COM : Click to view the full PDF of j2868_201010

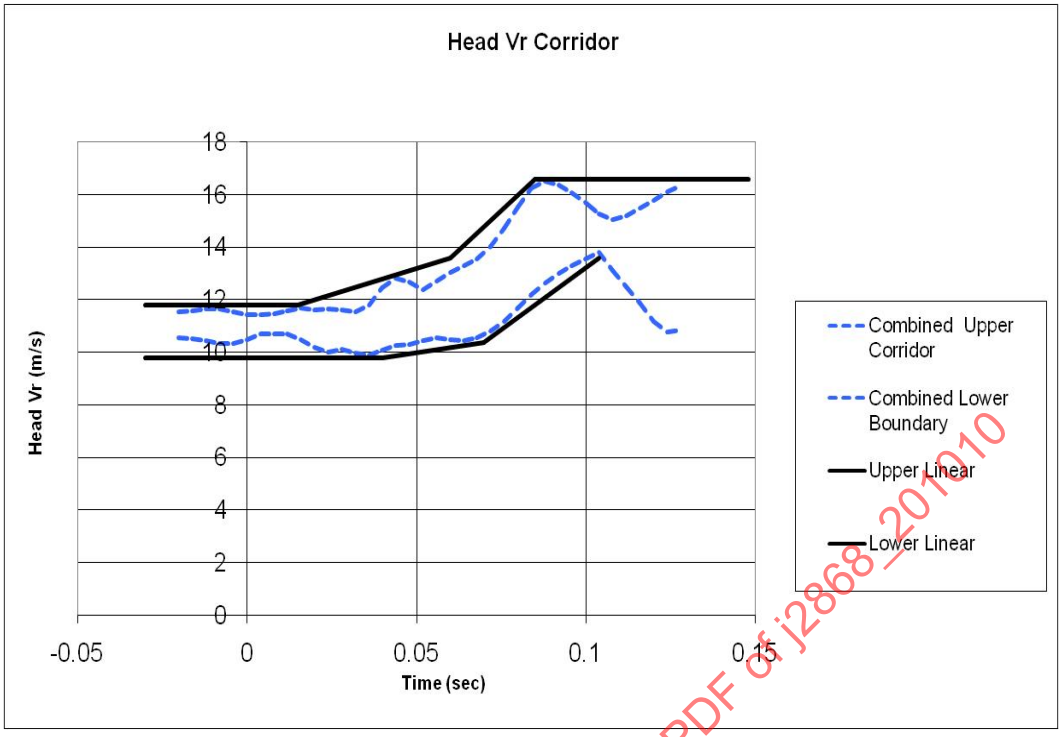

FIGURE 19 - FINAL HEAD VELOCITY CORRIDOR AND PIECEWISE LINEAR CORRIDOR

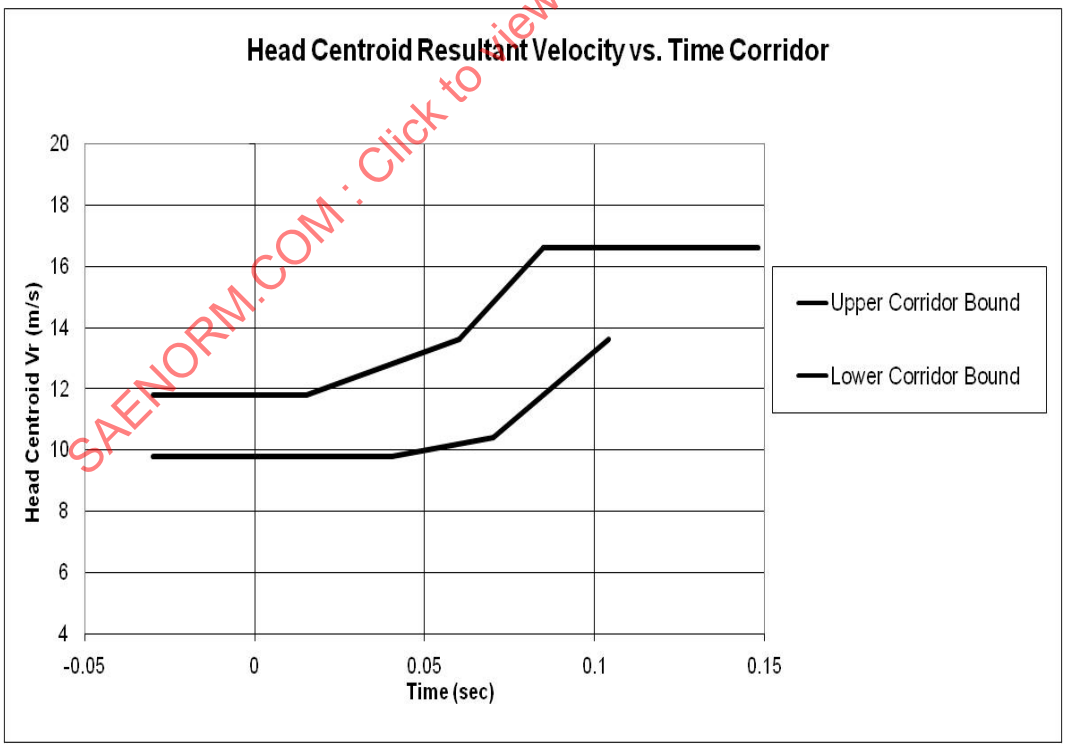

FIGURE 20 - HEAD CENTROID xz RESULTANT VELOCITY CORRIDOR
(IN VEHICLE REFERENCE FRAME)

NOTE: The head centroid velocity corridor can be plotted with the values in Table 10.

SAENORM.COM : Click to view the full PDF of j2868_201010

TABLE 10 - HEAD CENTROID xz RESULTANT VELOCITY CORRIDOR

Point	Upper Bound		Lower Bound	
	t(s)	V_r(m/s)	t(s)	V_r(m/s)
1	-0.030	11.8	-0.030	9.8
2	0.015	11.8	0.040	9.8
3	0.060	13.6	0.070	10.4
4	0.085	16.6	0.104	13.6
5	0.148	16.6	-	-

4. COMPARISONS BETWEEN EXISTING DUMMY TECHNOLOGY PERFORMANCE AND THE SPECIFICATIONS OF SAE J2782

One of the overall goals during the development of SAE J2782 was to establish performance goals which could be met by existing technologies. During the development and evaluation of the pedestrian dummy performance criteria found in SAE J2782, three candidate dummies were identified as current technology for conducting full-scale pedestrian impact tests. These dummies included the Hybrid-II frontal crash dummy with modified sit/stand pelvis and a lateral bending knee structure [Pritz, SAE 1978]; the Autoliv pedestrian dummy [Fredriksson, ESV 2001]; and the Polar-II [Akiyama, ESV 2001]. Each of these dummies was actively being used in the development of pedestrian protection systems at the time this Task Force activity commenced. All participants in the Task Force were invited to include their full-scale pedestrian dummies in the test and evaluation activity associated with development of the performance criterion. Honda volunteered to make the Polar-II available for round robin testing and Nissan presented data from tests with their Hybrid-II, but otherwise other dummies were not introduced for inclusion in this activity. Therefore, the Polar-II has primarily been used to demonstrate the ability of existing technology to achieve the performance criteria.

The intent of the following information is not to imply endorsement of any particular dummy or design but to demonstrate that the requirements of SAE J2782 can be satisfied with existing technologies.

4.1 Anthropometry Performance

The anthropometry performance specified in SAE J2782 Section 3 can of course be met if these were the only performance requirements, but design compromises created by other performance criteria may make it difficult to meet all of the specified criteria. The ability of exiting technologies to meet the criteria was evaluated using the Hybrid III and Polar-II dummies. A summary of SAE J2782 anthropometry requirements and recommendations and Hybrid III and Polar-II measures in shown in Table 11.

Table 11 provides many anthropometry measures for the dummy that require a shoe to be worn. It is assumed that shoes meeting the mass specifications given in SAE J2782 can be worn by the different dummy designs or the mass can be incorporated with the foot into a molded foot design. If the shoes are independent of the foot molding, the shoes utilized in the PMHS test (Kerrigan et al., ESV 2005) should meet have inertial properties of Ixx = 0.001001 kgm^2, Iyy = 0.003806 kgm^2, and Izz = 0.003899 kgm^2 relative to the center of gravity located in the foot (x = - 0.1434 m, y = - 0.0003 m, z = +0.0421 m) measured relative to an origin defined at the intersection of a plane containing the plane of the floor (XY Plane) and a plane perpendicular to the floor and tangent to the most posterior point of the shoe heel (YZ plane).

SAENORM.COM : Click to view the full PDF of j2868_201010

TABLE 11 - DUMMY COMPLIANCE WITH SAE J2782

	Anthropometry Specification	Specified Value			Specified Value		Required or Recommended	HIII with shoes	Polar II with shoes	HIII Complies	Polar Complies
		Target	+/- Tol.	Source	Min	Max					
Body Segment Mass (kg)	Head mass	4.1	0.2	AMVO	3.9	4.3	Recommended	4.53	4.5	No	No
	Neck mass	1.0	0.05	AMVO	0.95	1.05	Recommended	1.54	2.4	No	No
	Thorax mass	23.8	1.2	AMVO	22.6	25	Recommended	17.19	18.4	No	No
	Two arms	3.5	0.2	AMVO	3.3	3.7	Recommended	3.99	4.34	No	No
	Two forearms and hands	4.0	0.2	AMVO	3.8	4.2	Recommended	4.53	4.52	No	No
	Abdomen	2.4	0.1	AMVO	2.3	2.5	Recommended		2.5		Yes
	Pelvis	11.4	0.6	AMVO	10.8	12.0	Recommended	23.04	12.7	No	No
	Two thighs	17.2	1.0	AMVO	16.2	18.2	Recommended	11.97	13.6	No	No
	Two Legs	7.2	0.4	AMVO	6.8	7.6	Recommended	8.55	6.6	No	No
	Ankles and feet	2.0	0.1	AMVO	1.901	2.1	Recommended	2.79	2.5	No	No
	Mass of assembled dummy (with DAS)	79.6	4.0	CAESAR	75.6	83.6	Required	78.15	81.2	Yes	Yes
	Mass of assembled dummy with stub arms (with DAS)	75.6	4.0	Calculated from above	71.6	79.6	Required	73.62	76.7	Yes	Yes
Body Segment Dimension(mm)	Head Height	234	12	AMVO	219	243	Recommended	222	237	Yes	Yes
	Head Breadth	153	9	Average CAESAR and ANSUR	144	162	Recommended	156	157	Yes	Yes
	Head Circumference	571	30	Average CAESAR and ANSUR	541	601	Recommended	575	586	Yes	Yes
	Head Length	198	10	Average CAESAR and ANSUR	188	208	Recommended	203	200	Yes	Yes
	Shoulder Breadth	489	25	Average CAESAR and ANSUR	464	514	Recommended	470	515	Yes	No
	Circumference at interscye	1015	50	Average CAESAR and ANSUR	965	1065	Recommended	984	1005	Yes	Yes
	Interscye distance	397	20	Average CAESAR and ANSUR	377	417	Recommended	311	356	No	No
	Hip circumference	1000	50	Average CAESAR and ANSUR	950	1050	Recommended	972	1038	Yes	Yes
	Bi-trochanteric breadth	363	18	Average CAESAR and ANSUR	345	381	Recommended	362	378	Yes	Yes
	Thigh Circumference	593	35	Average CAESAR and ANSUR	558	628	Recommended	534	548	No	No
	Knee circumference	383	20	Average NASA and ANSUR	363	403	Recommended	410	400	No	Yes
	Maximum leg circumference	372	20	Average AMVO and ANSUR	352	392	Recommended	391	390	Yes	Yes
Body Segment CG (mm)**	Head	1697	35	AMVO	1662	1732	Recommended	1608	1646	No	No
	Neck	1564	50	AMVO	1514	1614	Recommended				
	Thorax	1293	75	AMVO	1218	1368	Recommended	1263	1289	Yes	Yes
	Arm	1305	75	AMVO	1230	1380	Recommended	1213	1281	No	Yes
	Forearm and hand	976	50	AMVO	926	1026	Recommended	995	1055	Yes	No
	Abdomen	1101	50	AMVO	1051	1151	Recommended				
	Pelvis	1024	50	AMVO	974	1074	Recommended	966	963	No	No
	Thigh	742	40	AMVO	702	782	Recommended	688	784	No	No
	Leg	353	20	AMVO	317	417	Recommended	311	315	No	No
	Foot	63	3	AMVO	60	66	Recommended				
Whole Body with shoes (mm)**	Distance from the bottom of the shoes to the top of the head	1785	15	Average AMVO, CAESAR, and ANSUR	1770	1800	Required	1714	1780	No	Yes
	Distance from the bottom of the shoes to the equivalent dummy location of T1	1542	15	Average AMVO, CAESAR, and ANSUR	1527	1557	Recommended		1469		No
	Distance from the bottom of the shoes to the center of rotation of the hip socket (H-point)	952	15	Average AMVO, CAESAR, and ANSUR	937	967	Recommended	924	936	No	No
	Distance from the bottom of the shoes to the center of rotation of the knee	527	15	Average CAESAR and ANSUR	512	542	Required	529	519	Yes	Yes
	Distance from the bottom of the shoes to the center of rotation of the ankle	99	5	Average CAESAR and ANSUR	94	104	Recommended	112	95	No	Yes
	Distance from the bottom of the shoes to the shoulder	1473	20	Average CAESAR and ANSUR	1453	1493	Recommended	1346	1456	No	Yes
	Distance from the bottom of the shoes to the elbow	1140	20	Average CAESAR and ANSUR	1120	1160	Recommended	1083	1160	No	Yes
	Distance from the bottom of the shoes to the wrist	881	20	Average CAESAR and ANSUR	861	901	Recommended	837	894	No	Yes
**	measured above the ground, standing erect with shoes and the arms at the sides										

SAENORM.COM : Click to view the full PDF of j2868_201010

4.2 Biofidelity Performance

4.2.1 Whole Dummy Response Performance

The ability of existing pedestrian dummy technology to meet the whole body response performance requirements specified in SAE J2782 was investigated using a Polar-II pedestrian dummy and the test procedures specified in SAE J2782. (2009). As detailed in Section 3 above, PMHS tests were performed and trajectory corridors were developed and the Polar-II dummy was then tested using the same vehicle and test procedures as is specified by SAE J2782. As is common practice, for this testing the Polar-II data was not scaled. When the Polar-II target locations did not correspond to the motion reference points defined in SAE J2782, Section 4.8.4.1.1.1, locations on the Polar-II corresponding to the motion reference points were “tracked” during the film analysis process. Figures 21 to 25 show that Polar-II performance meets the head, upper spine, mid thorax and pelvis trajectory and head velocity corridors.

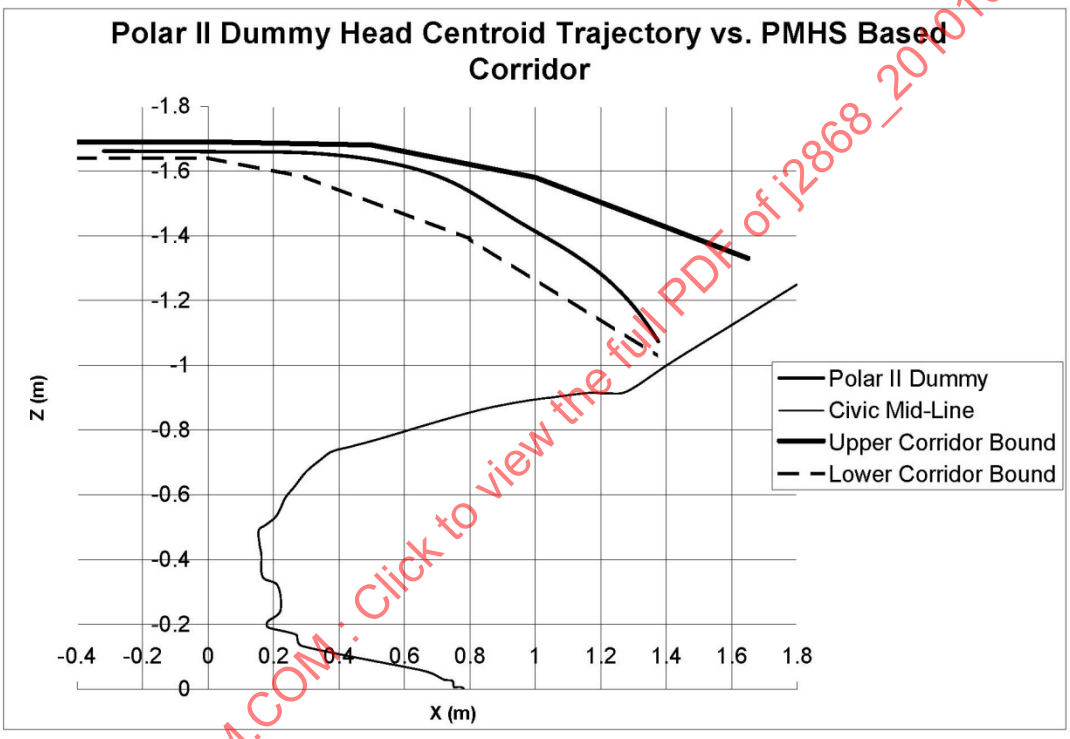

FIGURE 21 - POLAR HEAD TRAJECTORY VERSUS PMHS-BASED CORRIDOR

SAENORM.COM : Click to view the full PDF of j2868_201010

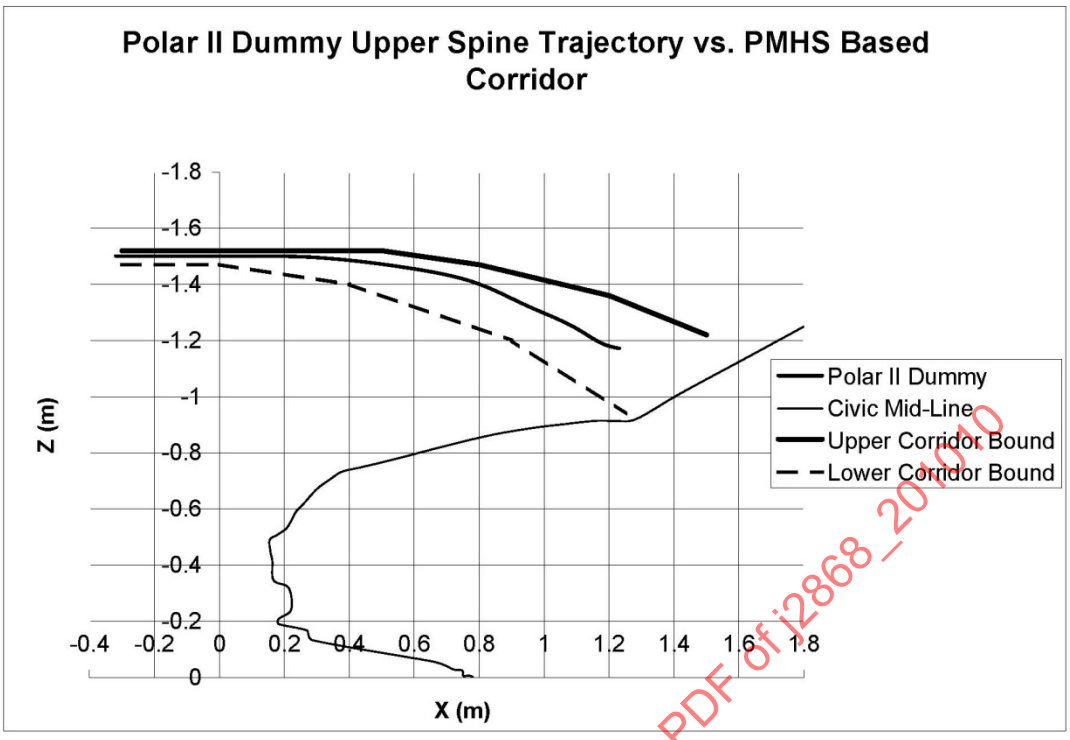

FIGURE 22 - POLAR UPPER SPINE TRAJECTORY VERSUS PMHS-BASED CORRIDOR

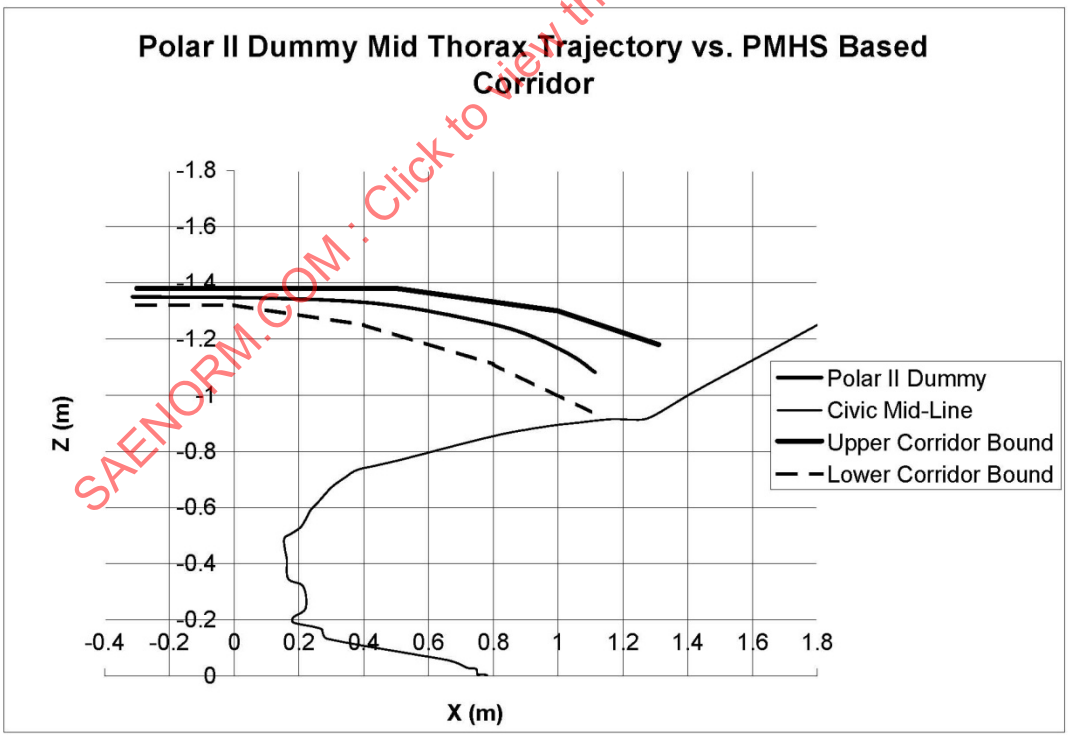

FIGURE 23 - POLAR MID THORAX TRAJECTORY VERSUS PMHS-BASED CORRIDOR

SAENORM.COM : Click to view the full PDF of j2868_201010

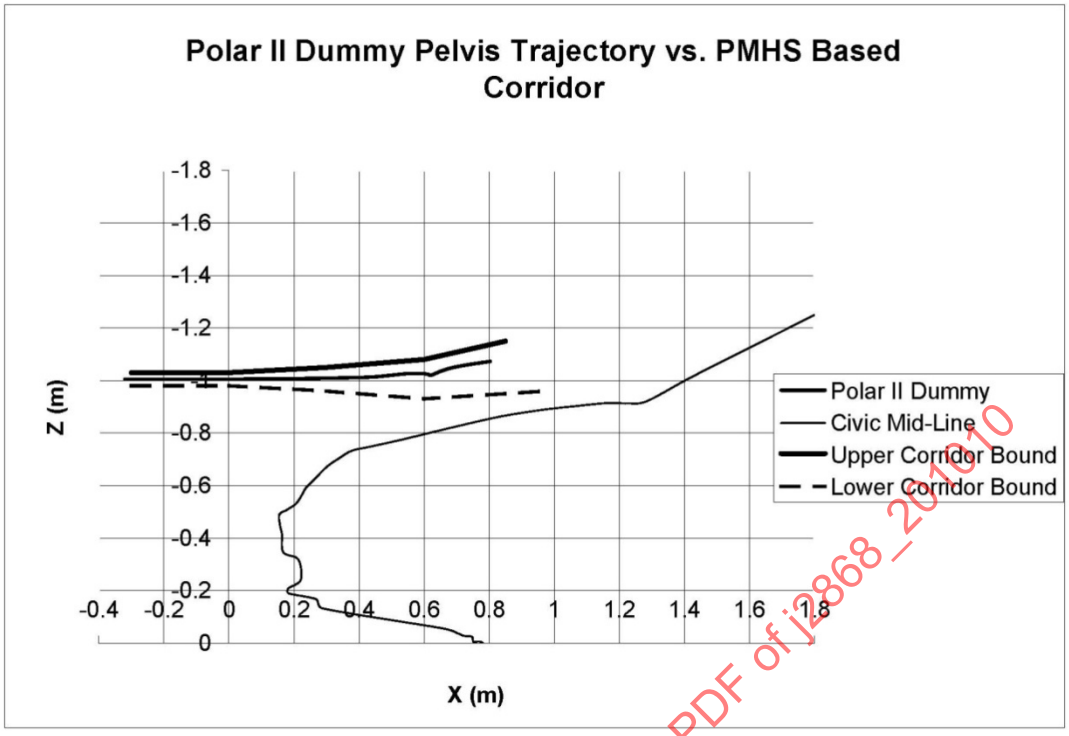

FIGURE 24 - POLAR PELVIS TRAJECTORY VERSUS PMHS-BASED CORRIDOR

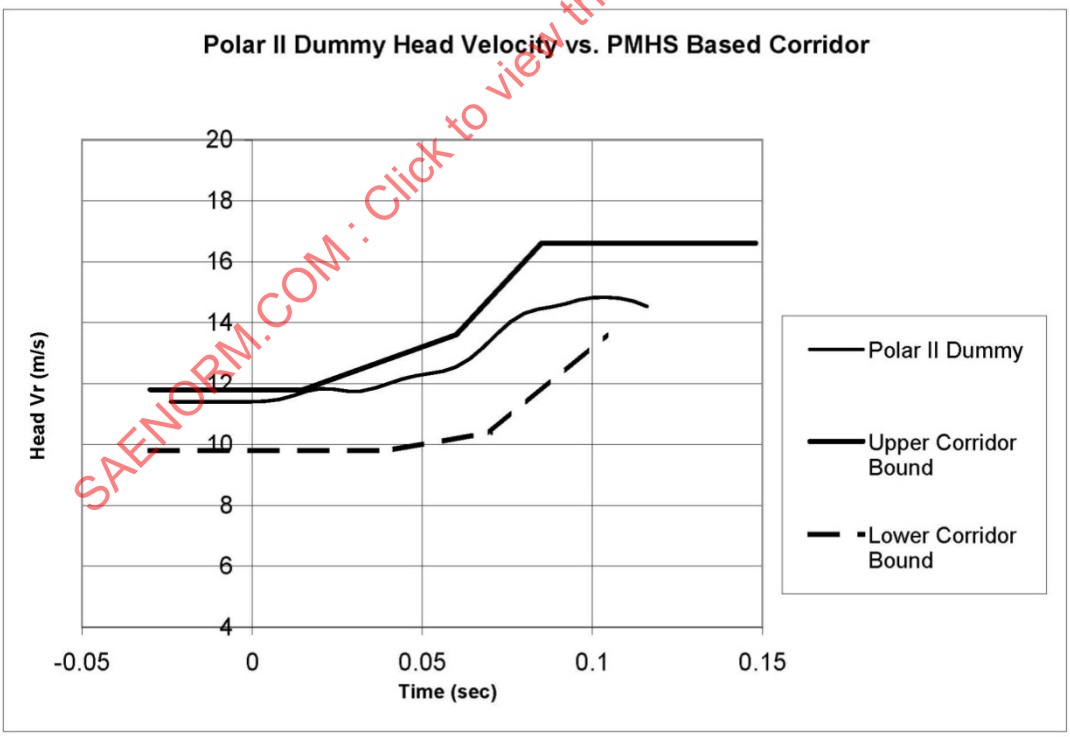

FIGURE 25 - POLAR HEAD CENTROID VELOCITY VERSUS PMHS-BASED CORRIDOR

SAENORM.COM : Click to view the full PDF of j2868_201010

4.2.2 Body Segment Responses Performance

4.2.2.1 Head and Neck

The ability of dummy head and neck assemblies to meet the frontal and lateral performance criteria outlined in FMVSS part 572 has long been established for ATDs such as the Hybrid-III and THOR. Current pedestrian dummies, such as Polar-II, use either modified Hybrid-III or THOR head/neck components and thus should be able to satisfy the head drop and neck pendulum performance requirements found in SAE J2782.

4.2.2.2 Shoulder

The ability to meet shoulder biofidelity specifications included in SAE J2782 Section 3.3.2 with existing technologies has been demonstrated by the 50th percentile male WorldSID design. As reported by Scherer (ESV 2009), the WorldSID shoulder lateral response falls within the required ISO/TR 9790:1999(E) Section 4.1.4 force/time corridor.

4.2.2.3 Thorax

Few existing ATDs are capable of meeting both frontal and lateral biofidelity criteria for the thorax. The thorax of the THOR Advanced Frontal Crash Test Dummy developed by GESAC, Inc and NHTSA however was developed to have some level of multidirectional biofidelity. As reported by White (SAFE 1996), in the 4.27 m/s frontal pendulum impact test THOR is able to fit in the 4.27 m/s frontal pendulum corridor (49CFR572.34) reasonably well. The Polar-II, which has a thorax construction based on THOR, was tested to the 4.3 m/s ISO/TR-9790 corridor for lateral biofidelity. The results of these tests showed that there was some lag in the initial ramp up of loading (Figure 26), but by making a small modification to the jacket foam the lateral response corridor could be satisfied (Figure 27).

SAENORM.COM : Click to view the full PDF of j2868_201010

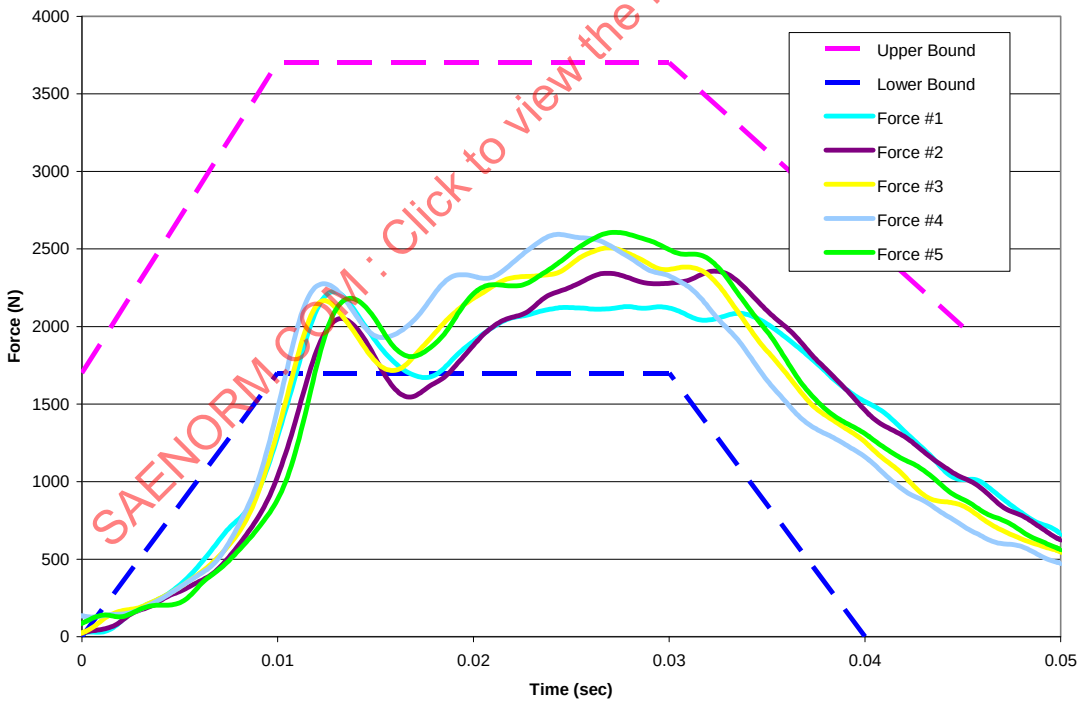

FIGURE 26 - BASELINE POLAR-II THORACIC RESPONSE IN THE 4.3 M/S LATERAL PENDULUM IMPACT

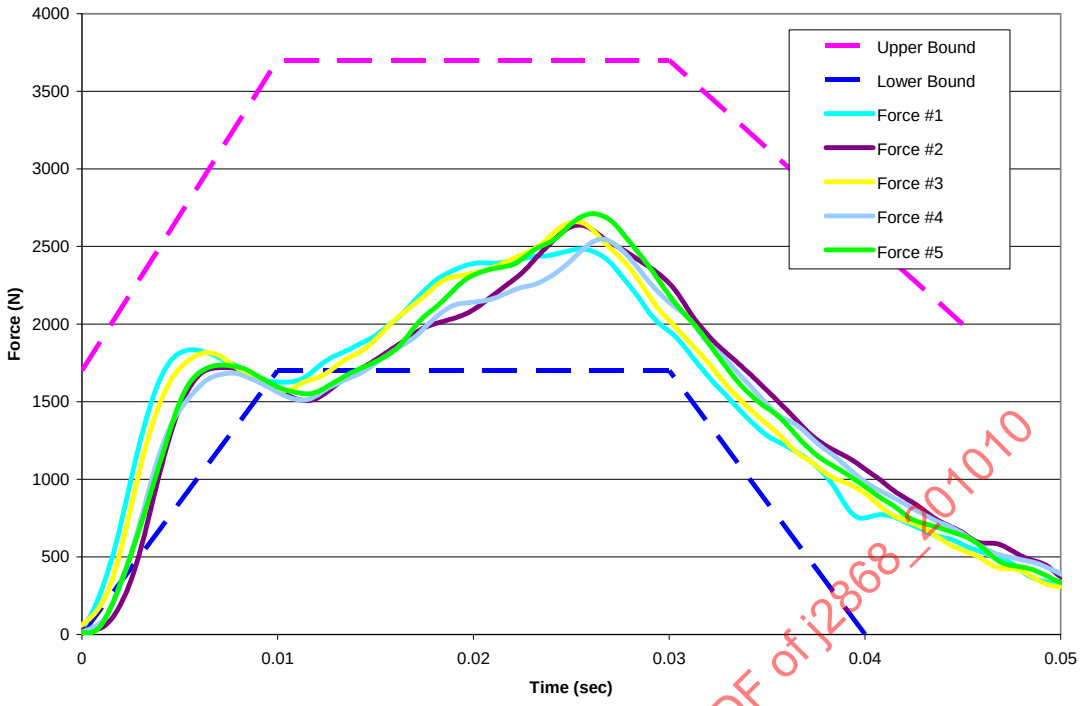

FIGURE 27 - MODIFIED POLAR-II THORACIC RESPONSE IN THE 4.3 M/S LATERAL PENDULUM IMPACT

4.2.2.4 Pelvis

The ability to meet pelvis biofidelity specifications included in SAE J2782 Section 3.6.2 with existing technologies has been demonstrated by the 50th percentile male WorldSID design. As reported by Scherer (ESV 2009), the WorldSID pelvis lateral response falls within the required ISO/TR 9790:1999(E) Section 4.3.4 force/velocity corridor when tested with a pendulum velocity of 6 m/s and is just slightly too stiff (force is slightly above the corridor) when tested at 10 m/s.

4.2.2.5 Knee

The ability of existing dummy designs to meet the SAE J2782 knee bending corridors was examined and verified by Takahashi, et al. (ESV 2005). While the original Polar-II knee fell within the lower bound of the corridor, it was deemed too compliant relative to the average PMHS moment-angle curve. Therefore, a modified Polar-II knee was developed by Takahashi et al. (ESV 2005) that exhibited moment-angle properties that provided a better approximation of the average PMHS knee response (see Figure 28) during the four-point bend tests.

SAENORM.COM : Click to view the full PDF of j2868_201010

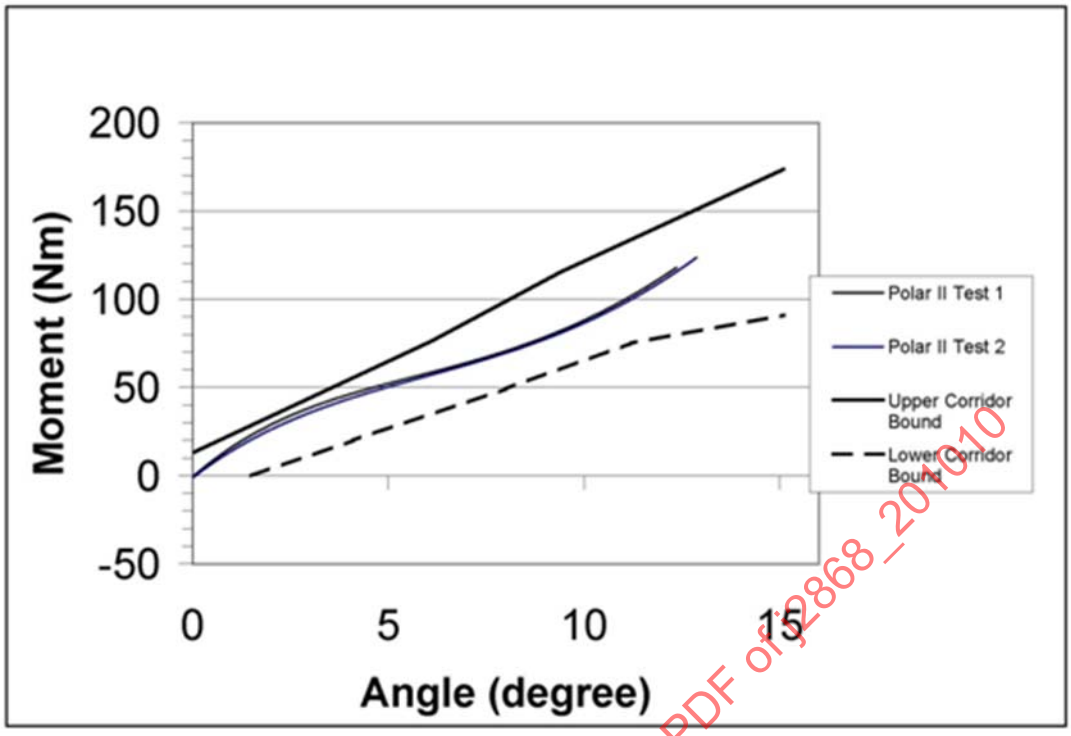

FIGURE 28 - MODIFIED POLAR-II KNEE STIFFNESS

4.2.2.6 Leg

The biofidelity of the Polar-II dummy leg in three-point bending was evaluated by Takahashi, et al. (ESV 2005). The Polar-II leg, when evaluated at the mid-shaft, fell within the upper and lower bounds (see Figure 29) of the idealized PMHS corridor specified in SAE J2782.

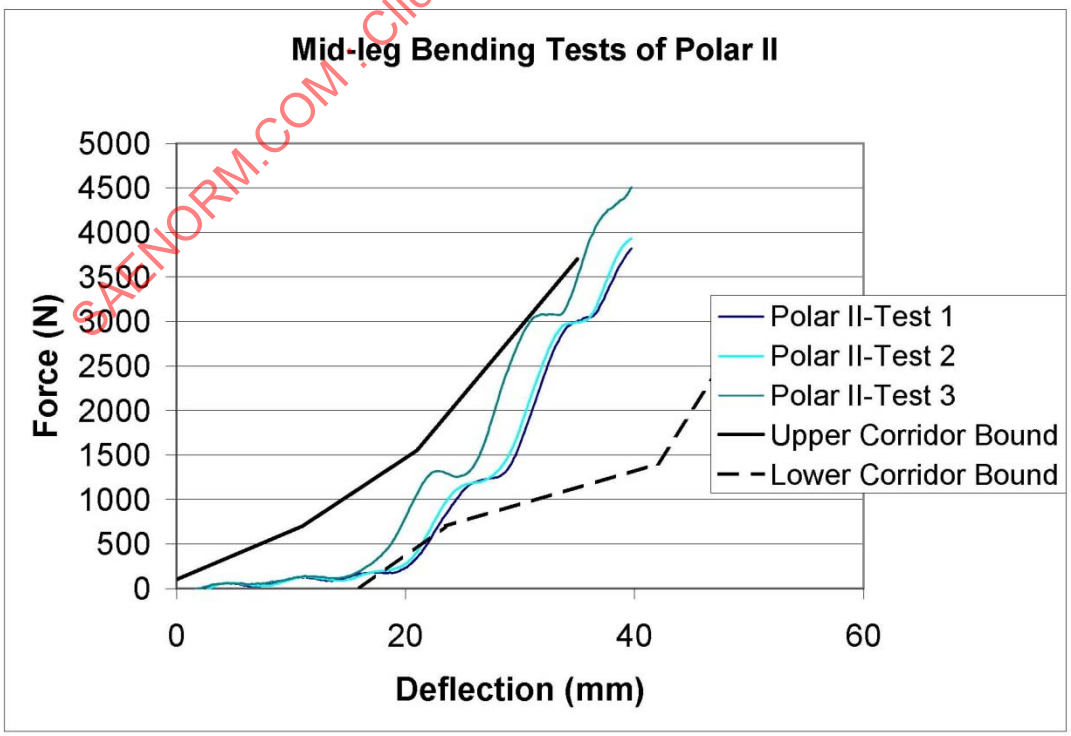

FIGURE 29 - POLAR-II LEG STIFFNESS

SAENORM.COM : Click to view the full PDF of j2868_201010

4.3 Instrumentation Availability

That the instrumentation requirements and sensor specifications in SAE J2782 Section 3 are compatible with existing dummy and sensor technologies can be verified by comparing the SAE J2782 Section 3 requirements to existing dummy technologies such as the WorldSID (as specified in ISO 15830), specialized motorcycle dummies (as specified in ISO 13232), the Polar-II pedestrian dummy (as specified in Polar-II User's Manual Version 2.2), and various occupant dummies and sensors offered by dummy and sensor manufacturers such as Robert A. Denton Inc., Denton ATD, Endevco, Entran, FTSS, and GESAC for example.

4.4 Repeatability and Reproducibility Performance

That the repeatability and reproducibility requirements of SAE J2782 Section 3 can be met by existing dummy technologies can be verified by comparing the requirements with measured WorldSID performance documented in ISO 15830. The WorldSID repeatability and reproducibility requirements are similar in scope and CV values to those specified for the pedestrian dummy in SAE J2782 and, as is documented in ISO 15830 the WorldSID, an example of existing dummy technology, met these performance requirements.

4.5 Durability Performance

The ability of existing dummy technologies to withstand the 50 km/h test specified in SAE J2782 Section 4 without sustaining non-cosmetic damage to non-frangible parts was demonstrated in a test performed with the Polar-II dummy (see Appendix D).

5. NOTES

5.1 Marginal Indicia

A change bar (l) located in the left margin is for the convenience of the user in locating areas where technical revisions, not editorial changes, have been made to the previous issue of this document. An (R) symbol to the left of the document title indicates a complete revision of the document, including technical revisions. Change bars and (R) are not used in original publications, nor in documents that contain editorial changes only.

SAENORM.COM : Click to view the full PDF of j2868_201010

PREPARED BY THE SAE PEDESTRIAN DUMMY TASK FORCE OF THE SAE HUMAN BIOMECHANICS AND SIMULATIONS STANDARDS STEERING COMMITTEE

APPENDIX A - TERMS OF REFERENCE OF THE SAE PEDESTRIAN DUMMY TASK FORCE

The following is a reprint of SAE Pedestrian Dummy Task Force Document TGN1 which is the final Terms of Reference for the Task Force.

Worldwide, pedestrian crashes constitute the most frequent cause of traffic-related fatalities. Knowledge about pedestrian crashes is essential to reduce fatality and injury of these vulnerable road users. Currently available tools and methods for studying pedestrian casualties include statistical databases, component testing, and computer simulations. Full-scale vehicle tests with a research dummy that is representative of a pedestrian are an essential component for understanding the mechanisms of pedestrian trauma and for developing appropriate countermeasures.

The near term aim of the Task Force is to develop performance specifications, for a pedestrian research dummy based on existing technology that can be used to study pedestrian-vehicle interactions. While the objective of the group is to develop performance specifications rather than a physical device, the Task Force realizes it is necessary to have a physical representation of such a research dummy in order to assess the feasibility of meeting the dummy performance specifications using existing technologies.

Possible uses of a pedestrian research dummy include the following:

- Design of countermeasures
- Evaluation of active systems (pop-up hoods, airbags, etc.)
- Validation of computer simulations
- Study of pedestrian kinematics
- Facilitate crash reconstruction including pedestrian kinematics
- Refine component test parameters and procedures
- Predict injury probabilities for given vehicle, crash, and countermeasure combinations
- Elucidate influence of pedestrian size on interaction, injury, and outcome

While it is recognized that collisions involve pedestrians of all sizes, it is proposed that performance specifications for a midsize adult male research dummy be developed as the first step. This approach stems from the greater knowledge of biomechanics and existing dummy technologies for the mid-size male relative to other adult sizes and children. While not the initial objective, it is envisioned that additional performance specifications for other sizes of pedestrian research dummies will be developed in the future based on accepted scaling procedures.

To develop pedestrian research dummy performance specifications that are based on existing technology, the following items must be undertaken by the TG:

- Biomechanical response requirements for a pedestrian research dummy - Biomechanical requirement should include size, mass, moment of inertia, static and dynamic responses of essential body regions. To determine these requirements, the literature should be surveyed and existing data should be gathered, classified, and consolidated.
- Certification procedures and requirement - Certification procedures to ensure that the production dummy designs meet biomechanical requirements.
- Instrumentation - Although injury criteria development is not a focus of this group, measurement of engineering parameters known to relate causally to injury is necessary for assessing injury potential of vehicle-pedestrian interactions. For this purpose, knowledge about the most frequent and severe pedestrian injuries must be combined with sensors containing appropriate engineering measures at critical body regions.
- Durability and repeatability - Durability and repeatability are essential characteristics of crash dummies. Establishing requirements will be necessary.
- Functionality - The specification should ensure ease of use in a crash-laboratory environment.
- Survey of existing technology - The establishment of performance specifications based on existing technologies will require a careful review and evaluation of existing pedestrian dummies and other dummy technologies, which may form the basis for the specifications.

The development of the performance specifications document shall be completed by June 2005.

SAENORM.COM : Click to view the full PDF of j2868_201010

APPENDIX B - EXPERT RANKINGS OF BODY REGION PRIORITIES

The following is a reprint of SAE Pedestrian Dummy Task Force Document TGN78 which includes information related to the expert ranking of pedestrian body region priorities (see Appendix C also).

In order to determine body region priorities for a variety of performance specifications including instrumentation compatibility, component biofidelity, and whole body kinematics for a dummy design, a detailed review of available field injury studies was undertaken. The study showed a variety of investigations detailing injury frequency, injury severity, injury cost, and disability probabilities. Attempts to objectively combine the results of the various studies were hampered by a lack of common procedures, terminology, and body segmentations. In order to prioritize body regions, a group of 10 experts, familiar with the available studies were asked to prioritize the body regions (1 = most important, 10 = least important) based on such factors as the frequency of injury to the body region, the societal cost associated with the injury, and the probability of disability. The results, shown in Table B-1, showed that the body regions could be combined into four priority groups (group A - most important and group D - least important). The results of the rankings are shown in Figure B1. Additional details describing the ranking procedures and results may be found in Appendix C.

TABLE B1 - BODY REGION PRIORITY

	Expert number	Priority Rankings										Total	Average	St. Dev	Necessity
		1	2	3	4	5	6	7	8	9	10				
Region															
head		1	1	1	1	1	1	1	1	1	1	10	1	0.00	A
knee		5	2	4	2	2	2	4	2	3	3	29	2.9	1.10	B
leg		2	7	2	3	4	5	2	6	2	2	35	3.5	1.90	B
thorax		4	3	3	4	3	3	3	4	4	5	36	3.6	0.70	B
cervical		3	5	7	10	8	6	8	3	5	4	59	5.9	2.33	C
pelvis		6	6	5	6	7	4	7	5	6	7	59	5.9	0.99	C
abdomen		6	4	6	7	5	8	5	8	7	6	62	6.2	1.32	C
femur		9	8	8	8	9	7	6	7	8	8	78	7.8	0.92	D
ankle foot		9	9	10	5	10	9	9	9	10	9	89	8.9	1.45	D
upper ext		6	10	9	9	6	10	10	10	9	10	89	8.9	1.60	D
	sum	51	55	55	55	55	55	55	55	55	55				

SAENORM.COM : Click to view the full PDF of j2868_201010

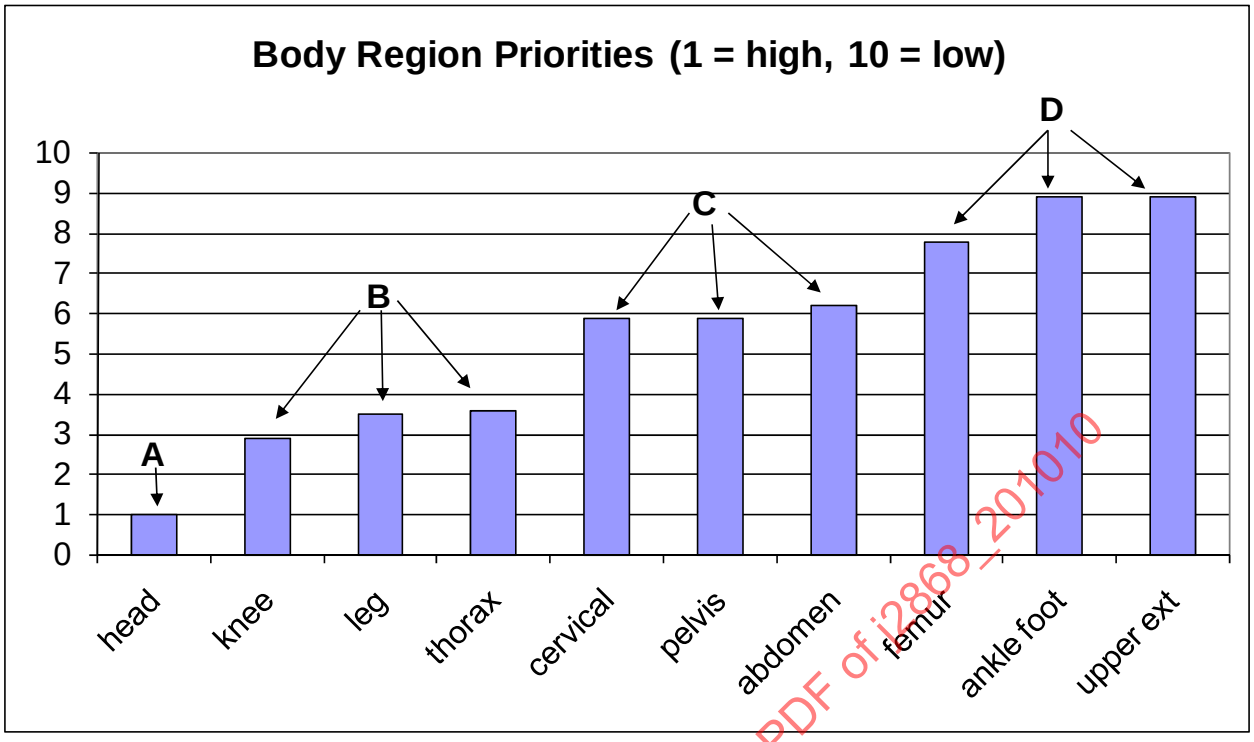

FIGURE B1 - BODY REGION PRIORITIES

Some example factors on which the above rankings were based included:

- Head injuries were the most frequent severe injuries
- Knee (including distal femur and proximal tibia) and leg injuries were the most frequent AIS 2 + injuries
- Cervical injuries, although not common are extremely costly and severe when they do occur
- Thorax injuries were of moderate frequency but high severity
- Upper extremity injuries were of moderate frequency and low severity

SAENORM.COM : Click to view the full PDF of j2868_201010

APPENDIX C - MINUTES OF THE 4TH SUB-GROUP MEETINGS OF THE SAE PEDESTRIAN DUMMY TASK FORCE

The following is a summary of SAE Pedestrian Dummy Task Force Document TGN86, with attendee names removed, which includes information related to the expert ranking of pedestrian body region priorities (see Appendix B also). In places, the excerpt below is not reprinted as approved and may contain corrections of spelling and typographical errors and other minor corrections noted after the approval of the original document.

Collectively, a group of experts met in Goteborg, Sweden on 9/8/2004 to determine body region priorities for the development of body region biofidelity and instrumentation requirements. Since the priorities for pedestrians may change over time, the appendix provides a summary of what was considered current at the time of writing of this information report. The available literature was reviewed that included published field data studies of pedestrian injuries. While age was a factor for the risk of pedestrian injury, no age breakdown of the injury data was considered when reviewing the occurrence of injuries and priorities. In general, head injuries were considered the most frequent serious injury while lower limb injuries were the most frequent AIS 2+ injuries.

A discussion regarding pedestrian dummy instrumentation requirements to monitor injuries by body region was undertaken by the group of experts. Knee motions were considered important, but three-dimensional joint rotations cannot be measured with existing technologies. The most common pelvis fracture is a fracture of the ramus. The forces required to cause a rami fracture differ with contact location. Fracture forces caused by trochanter contact are different than fracture forces caused by iliac crest contact. The pelvis instrumentation available in the WorldSID was discussed. The ability to place 6 axis load cells above and below the knee and perform post-test calculations of knee three-dimensional rotations was discussed. The possible use of small load cells to measure knee ligament cables was discussed. Measurements should be made which are as close to the injury mechanism as possible, (e.g. if the knee injury mechanism is ligament tension, dummy ligament tension measurements would be better than joint rotations, assuming the dummy joint is representative of human geometry). For thorax deflection measurements, it is difficult to measure the absolute maximum deflection because in pedestrian testing, which involves three dimensional motions, the direction and location of the maximum deflection is impossible to predict prior to the test. "Bony thorax" is the term used to refer to the region covered by the rib cage. This includes the liver, spleen, and other internal organs normally associated with the abdomen. From a practical standpoint, injuries to these organs frequently involve rib deflections so from an injury measurement standpoint will be included as the bony thorax. In terms of local deformation, heart injuries are generally at the level of 4th rib deflections (lateral) and liver injuries are at the level of the lateral 8th rib deflections. Dummy thorax deflection sensors should be located so as to measure displacements corresponding to the location of human 4th and 8th ribs. From discussions at prior meetings, the priorities (5 is high priority, 0 low) for instrumentation by body region was head 5, cervical spine 3, thorax 4, abdomen 3, pelvis 3, (the femur, knee, and tibia were listed as "high" but no numerical value was previously assigned). Discussions related to lower limb injuries included a review of lower limb injury data in the literature that showed some inconsistencies related to the classifications of injuries and injury locations. Some studies discussed AIS-based anatomical injuries rather than their function role. For example, fractures to the top of the tibia tend to be listed as tibia injuries rather than knee injuries. When based on anatomical descriptors, knee injuries tend to show a slightly lower occurrence than leg or femur injuries.When reviewed by functional or regional descriptions, the proximal and distal ends of bones are grouped with the joint rather than with the general descriptor of the particular bone or segment. In this case, the occurrence of thigh injuries decreases and knee injuries increase because injuries to the end of the femur are classified as joint or knee injuries. It was proposed that the Task Force review injuries by function or location.

SAENORM.COM : Click to view the full PDF of j2868_201010

Knee injuries would include injuries to the:

- Femoral condyle
- Patella
- Ligament
- Dislocations
- Tibial plateau

Femur injuries would include injuries to the shaft only.

Based on functional definitions lower extremity injury occurrence rankings would be:

- Tibia (1)
- Knee (2)
- Pelvis (3)
- Ankle (4)
- Femur (5)

When considering both frequency of occurrence and severity, the lower extremity priorities might be:

- Pelvis 3
- Femur 2.5
- Knee 4.5
- Leg 3.5
- Ankle 2

Femur and pelvis injuries may decrease when hood height is decreased as this has been shown by vehicles in the 1990s and with more recent LTV, hood radius is increased, or bumper height is increased.

Given the wide variation in field data studies including inclusion criteria, body region grouping, injury severities investigated, etc., discussion of the relative importance of biofidelity for various body regions based on injury severity and frequency of occurrence was done using a subjective interpretation of the literature by a panel of experts. Based on all data reviewed and discussed, each of the ten experts present were asked to rate the importance of each of the body regions using a 10 point scale (1 highest priority, 10 lowest priority). The body regions were:

- Head
- Cervical
- Thorax
- Abdomen
- Pelvis
- Femur
- Knee
- Leg
- Ankle
- Upper extremities

The ratings from all ten experts were averaged. Regions with similar ratings were grouped. The results are as follows (also see TG-N78).

- Head = 1.0 (Group A) (highest priority on a scale of 1 to 10)
- Knee = 2.9 (Group B)
- Leg = 3.5 (Group B)
- Thorax = 3.6 (Group B)
- Cervical = 5.9 (Group C)
- Pelvis = 5.9 (Group C)
- Abdomen = 6.2 (Group C)
- Femur = 7.8 (Group D)
- Ankle foot = 8.9 (Group D)
- Upper extremity = 8.9 (Group D)

SAENORM.COM : Click to view the full PDF of j2868_201010

APPENDIX D - POLAR –II 50 KM/HR TEST RESULTS

The following is a black and white reprint of SAE Pedestrian Dummy Task Force Document TGN109 which includes a brief overview of the results of a 50 km/h impact test designed to investigate the durability of existing dummy designs.

The objective was to evaluate the durability of the Polar II dummy at a nominal impact speed of 50 km/h. The test conditions included a 2004 Honda Civic Sedan. The dummy was struck laterally and was suspended by a release mechanism that was released 30 ms prior to impact. Braking of the vehicle was applied 200 ms after impact. The ground surface where the dummy was intended to land was covered with padding to avoid any damage from the dummy from occurring from the ground rather than the vehicle.

FIGURE D1 - TEST CONFIGURATION FOR POLAR II DURABILITY TESTING

The actual impact speed was 50.5 km/h. Following the test, no damage to the structural parts or the instrumentation were noted. A few cuts of the dummy head skin were sustained from the vehicle windshield.

FIGURE D2 - VEHICLE DAMAGE FOLLOWING POLAR II DURABILITY TESTING

SAENORM.COM : Click to view the full PDF of j2868_201010